



HAL
open science

Genomics accelerated isolation of a new stem rust avirulence gene–wheat resistance gene pair

Narayana M Upadhyaya, Rohit Mago, Vinay Panwar, Tim Hewitt, Ming Luo, Jian Chen, Jana Sperschneider, Hoa Nguyen-Phuc, Aihua Wang, Diana Vallejo Ortiz, et al.

► **To cite this version:**

Narayana M Upadhyaya, Rohit Mago, Vinay Panwar, Tim Hewitt, Ming Luo, et al.. Genomics accelerated isolation of a new stem rust avirulence gene–wheat resistance gene pair. *Nature Plants*, 2021, 7 (9), pp.1220-1228. <10.1038/s41477-021-00971-5>. <hal-03906041>

HAL Id: hal-03906041

<https://hal.science/hal-03906041v1>

Submitted on 2 Oct 2024

HAL is a multi-disciplinary open access archive for the deposit and dissemination of scientific research documents, whether they are published or not. The documents may come from teaching and research institutions in France or abroad, or from public or private research centers.

L'archive ouverte pluridisciplinaire **HAL**, est destinée au dépôt et à la diffusion de documents scientifiques de niveau recherche, publiés ou non, émanant des établissements d'enseignement et de recherche français ou étrangers, des laboratoires publics ou privés.



HAL Authorization

1 **Genomics accelerated isolation of a new stem rust avirulence gene**
2 **- wheat resistance gene pair**

3

4 Narayana M. Upadhyaya^{1*}, Rohit Mago^{1*}, Vinay Panwar², Tim Hewitt¹, Ming Luo¹, Jian
5 Chen^{1,3}, Jana Sperschneider⁴, Hoa Nguyen-Phuc⁵, Aihua Wang¹, Diana Ortiz^{1,#}, Luch Hac¹,
6 Dhara Bhatt¹, Feng Li⁶, Jianping Zhang¹, Michael Ayliffe¹, Melania Figueroa¹, Kostya
7 Kanyuka², Jeffrey G. Ellis¹, Peter N. Dodds^{1**}

8

9 ¹ Commonwealth Scientific and Industrial Research Organisation, Agriculture and Food,
10 GPO Box1700, Canberra, ACT 2601, Australia

11 ² Biointeractions and Crop Protection, Rothamsted Research, Harpenden, AL5 2JQ, United
12 Kingdom

13 ³ Research School of Biology, Australian National University, Canberra ACT 2601, Australia

14 ⁴ Biological Data Science Institute, The Australian National University, Canberra, ACT 2601,
15 Australia

16 ⁵ Department of Ecology and Evolutionary Biology, Vietnam National University, 227
17 Nguyen Van Cu Street, District 5, HCMC, Vietnam

18 ⁶ Department of Biomedical Statistics and Informatics, Mayo Clinic, Rochester, Minnesota
19 55905, USA

20

21 * These authors contributed equally

22 ** author for correspondence: peter.dodds@csiro.au

23

24 # current address: Génétique et Amélioration des Fruits et Légumes (GAFL), INRA,
25 Domaine Saint Maurice, 63 Allée des Chênes, CS60094, 84143 Montfavet Cedex, France

26 Stem rust caused by the fungus *Puccinia graminis* f. sp. *tritici* (*Pgt*) is a devastating disease
27 of the global staple crop wheat. Although this disease was largely controlled by genetic
28 resistance in the latter half of the 20th century, new strains of *Pgt* with increased virulence, such
29 as Ug99, have evolved by somatic hybridisation and mutation ^{1,2}. These newly emerged strains
30 have caused significant losses in Africa and other regions and their continued spread threatens
31 global wheat production. Breeding for disease resistance provides the most cost-effective
32 control of wheat rust diseases ³. A number of race-specific rust resistance genes have been
33 characterised in wheat and most encode immune receptors of the nucleotide-binding leucine-
34 rich repeat (NLR) class ⁴. These receptors recognize pathogen effector proteins often known as
35 avirulence (*Avr*) proteins ⁵. However, only two *Avr* genes have been identified in *Pgt* to date,
36 *AvrSr35* and *AvrSr50* ^{6,7} and none in other cereal rusts, which hinders efforts to understand the
37 evolution of virulence in rust populations ^{8,9}. The *Sr27* resistance gene was first identified in a
38 wheat line carrying an introgression of the 3R chromosome from Imperial rye ¹⁰. Although not
39 deployed widely in wheat, *Sr27* is widespread in the artificial crop species *Triticosecale*
40 (triticale) which is a wheat-rye hybrid and is a host for *Pgt* ^{11,12}. *Sr27* is effective against Ug99
41 ¹³ and other recently emerged *Pgt* strains ^{14,15}. Here we identify both the *Sr27* gene in wheat
42 and the corresponding *AvrSr27* gene in *Pgt* and show that virulence to *Sr27* can arise
43 experimentally and in the field through deletion mutations, copy number variation and
44 expression level polymorphisms at the *AvrSr27* locus.

45 The wheat stem rust isolate Pgt21-0 is avirulent on *Sr27*, but derivatives of this strain with
46 virulence to *Sr27* have been detected in the field ^{16,17}, suggesting that it may be heterozygous
47 for *AvrSr27*. We therefore selected for spontaneous virulent rust mutants after inoculation of
48 Pgt21-0 onto the resistant triticale cultivar ‘Coorong’ carrying *Sr27*. Three large single pustules
49 were selected, purified in isolation and reinoculated onto Coorong to confirm their virulent
50 phenotype (Fig. 1A and Supplementary Fig. 1). We generated Illumina sequence data from
51 genomic DNA of each mutant and mapped the reads to the Pgt21-0 haplotype-resolved genome
52 assembly ² to identify potential mutations. We first screened for SNPs causing amino-acid
53 changes in secreted protein genes, but found no genes with such mutations in more than one
54 mutant line. Next we looked for loss of read coverage as an indicator of potential deletion
55 mutations. Each of the mutant lines showed a large number of genes with zero read coverage,
56 all located on one end of chromosome 2B. Visualisation of read mapping depth to chromosome
57 2B revealed the three mutants each contained independent and overlapping deletions (Fig. 1B).
58 The largest was 1.5Mbp in size and corresponds to the whole of the short arm of this

59 chromosome. The smallest common deleted region was 196kbp and contains 50 annotated
60 genes, five of which are predicted to encode secreted proteins (Fig. 1C).

61 We previously sequenced two Australian *Pgt* isolates (Pgt34-2,12 and Pgt34-2,12,13) that
62 are clonally derived from Pgt21-0 and had evolved virulence for *Sr27* in the field ^{16,17}. Analysis
63 of read coverage revealed that these two isolates each contained a small deletion of 13 kbp in
64 the same region of chromosome 2B that was deleted in the three spontaneous mutants. This
65 small deletion spanned two of the secreted protein genes (PGT21_006532 and PGT21_006593)
66 along with a single adjacent gene on the distal side (Fig. 1C and Supplementary Fig. 2). No
67 other genes in this region contained any changes in these two isolates. We confirmed the
68 presence of this deletion in the genome of Pgt34-2,12 by PCR amplification of the deletion
69 boundaries (Supplementary Fig. 3). We also examined sequence data previously generated
70 from seven South African isolates ¹⁸ that are part of the same clonal lineage as Pgt21-0 ^{2,19}.
71 Pgt21-0 migrated to Australia from South Africa and was first detected in 1954, and these two
72 branches of this lineage have since evolved in isolation. Four of the South African isolates
73 examined are virulent on *Sr27* ²⁰ and must have evolved this phenotype independently of the
74 Australian isolates. Sequence analysis revealed that three of these virulent lines each contain
75 an identical ~14kbp deletion that overlaps with the deletion in Pgt34-2,12 and spans the two
76 candidate secreted protein genes plus an additional gene on the proximal side, while the fourth
77 isolate contains an independent deletion of 10 kbp that spans just the two secreted protein genes
78 (Fig. 1C and Supplementary Fig. 2). Importantly all five of the avirulent isolates of this lineage
79 contain a similar sequence to Pgt21-0 in this region (Fig 1C). A phylogenetic analysis of these
80 clonal isolates places each unique deletion event in a separate branch, consistent with three
81 independent mutations to virulence on *Sr27* during the diversification of this lineage
82 (Supplementary Fig. 4). The deletion of these two secreted protein gene candidates in three
83 independent field-derived virulent lineages provides strong evidence that at least one of these
84 genes confers the *AvrSr27* avirulence phenotype.

85 The two *AvrSr27* candidate genes are closely related to each other and encode predicted
86 secreted proteins of 144 amino acids designated *AvrSr27-1* and *AvrSr27-2* (Fig. 2A). A single
87 copy of a related gene (PGT21_007034) occurs at the alternate (virulence) allele on
88 chromosome 2A (designated *avrSr27-3*) and the three protein variants differ at 35 amino acid
89 positions. These proteins show no similarity to any proteins from other rust species. To test the
90 avirulence function of these proteins, we generated recombinant *Barley stripe mosaic virus*
91 (BSMV) ²¹ expressing the *AvrSr27* candidates without their predicted signal peptides. We

92 found that BSMV expressing any of the three *AvrSr27* variants was unable to infect the triticale
93 line Coorong, while the control virus vector (BSMV:mcs4d) carrying a 275-nt noncoding DNA
94 fragment was highly infective (Fig. 2B, Supplementary Fig. 5a). All BSMV strains could infect
95 the rust susceptible triticale line Rongcoo. We further tested these strains for infection of an
96 EMS derived mutant of Coorong that had lost *Sr27* resistance (see below). All were able to
97 infect this line, indicating that recognition was specifically conferred by the *Sr27* resistance
98 gene (Fig. 2B, Supplementary Fig. 5a). Furthermore, BSMV strains expressing
99 PGT21_006334 (another secreted protein candidate in the M1 196kbp deletion but outside the
100 small deletions) were fully able to infect Coorong indicating that recognition was specific to
101 the *AvrSr27* candidates. We also tested *AvrSr27* recognition in the wheat line Chinese Spring
102 WRT238.5, containing the 3RS translocation carrying *Sr27*. BSMV strains expressing *AvrSr27*
103 variants could not infect WRT238.5 containing *Sr27* but could infect the susceptible line
104 Chinese Spring (Supplementary Fig. 5b).

105 It was unexpected that the *avrSr27-3* variant from the virulence allele also conferred
106 recognition by *Sr27* in these assays. This allelic variant did not contain any sequence changes
107 in any of the *Sr27*-virulent isolates examined. Thus, there must be some reason apart from the
108 amino acid differences in the mature protein that explains the lack of an avirulence phenotype
109 conferred by this allele in *Pgt*. One possibility is that expression level differences between the
110 variants may explain this phenotype. We therefore analysed Illumina RNAseq data from an
111 infection time course and isolated haustoria of Pgt21-0⁶ mapped to the Pgt21-0 annotated
112 genome². This analysis showed that the *AvrSr27-2* variant (PGT21_006593) was expressed
113 approximately four-fold higher than the other two variants (Fig. 3A) and therefore likely
114 contributes most to avirulence during infection of *Sr27* plants. Notably, we found that the
115 *avrSr27-3* variant on chromosome 2A (retained in virulent isolates) accounts for only about
116 15% of the total expression from this locus. We hypothesise that this could be below a threshold
117 required to confer an avirulence phenotype in the absence of the other two variants encoded on
118 chromosome 2A. Consistent with this, RT-PCR analysis confirmed that the combined
119 expression at the *AvrSr27* locus was substantially reduced in the virulent *Pgt* mutant #1
120 compared to the wildtype avirulent Pgt21-0 (Supplementary Fig. 6). Effector expression level
121 polymorphisms rather than protein sequence variation were also observed to underlie virulence
122 in some *Phytophthora spp.* isolates^{22,23}. Cluster analysis of expression profiles of all secreted
123 protein genes in Pgt21-0 revealed eight clusters with different expression profiles in germinated
124 spore, haustoria and in infected leaves (Fig. 3B). Clusters 2, 3 and 7 are characterised by

125 upregulated expression in haustoria relative to germinated spores and early expression during
126 plant infection. Cluster 6 includes haustorially enriched genes that are induced late during
127 infection, while genes in clusters 1, 5 and 8 are preferentially expressed in germinated spores
128 and cluster 4 included genes with relatively stable expression. The three known Pgt *Avr* genes
129 shared a similar expression pattern and appear in clusters 2 (*AvrSr35*) and 7 (*AvrSr27* and
130 *AvrSr50*). This shared expression profile is similar to that observed for six confirmed *Avr* genes
131 identified in the flax rust pathogen *Melampsora lini*²⁴, supporting the use of expression
132 profiling to prioritise candidate genes for avirulence function in rust fungi.

133 We also examined the *AvrSr27* locus in the reference sequence of Ug99², which is avirulent
134 on *Sr27* plants¹³. The A genome haplotype of Ug99 is shared with 21-0 and contains an
135 identical sequence to the virulence allele *avrSr27-3* (PGTUg99_032104). The C genome
136 haplotype (contig #00000029) encodes two proteins, one identical to *AvrSr27-2* (not
137 annotated) and one with a single amino acid difference from *AvrSr27-1* (PGTUg99_024168).
138 However, this genome region is distinguished from the Pgt21-0 chromosome 2B haplotype by
139 the presence of two large insertions (7 kbp and 9 kbp) and a duplication of about 1.5 kbp within
140 the intergenic region between the *AvrSr27* paralogs (Supplementary Fig. 7). Hence the Ug99
141 strain is also likely heterozygous for avirulence on *Sr27* plants.

142 We used a MutRenSeq²⁵ approach to identify the *Sr27* gene. Seeds of the triticale variety
143 Coorong carrying *Sr27* were treated with EMS and 1960 M2 families were screened for
144 susceptible mutants by infection with the avirulent Pgt21-0. A total of 35 putative mutants were
145 identified and 27 were subsequently confirmed in the following generation as homozygous
146 susceptible (Fig. 4A). NLR-gene capture and sequencing was performed on wildtype Coorong
147 and four confirmed susceptible mutants (M2, M3, M4 and M6). Sequence reads from Coorong
148 were assembled and reads from all lines aligned to this reference to identify sequence changes
149 in the mutant lines. One contig (#5723) of 1126 bp was found that contained a mutation in three
150 of the four mutants; one (M2) with a full deletion of the sequence and two (M3, M4) with single
151 base changes causing amino acid substitutions Q264R and G209S (in the conserved p-loop).
152 This contig contained a coiled-coil (CC) domain and p-loop motif, but not the rest of the NB-
153 ARC or LRR domains, suggesting that it represented only part of a full length NLR gene. To
154 identify the remainder of the gene, the contig was aligned to the *Triticum aestivum* cv. Chinese
155 Spring reference (CSv1) assembly IWGSC RefSeq v1.0²⁶. The top hit (93.6%) was to the
156 5' end of a high confidence gene (TraesCS6B01G464400) predicted on chromosome 6B and
157 functionally annotated as a disease resistance gene. The full gene sequence of

158 TraesCS6B01G464400 was then aligned back to the Coorong RenSeq *de novo* assembly which
159 detected an additional contig (#2413) aligning to the 3' region of this gene with 93.8% identity.
160 Contig #2413 contained both an NB-ARC and LRR domain, and inspection of the mutant line
161 read alignments confirmed that it was also deleted in mutant M2 and identified an additional
162 single base change in mutant M6 (Supplementary Fig. 8). PCR amplification from genomic
163 DNA confirmed that these two contigs are derived from the same gene in Coorong. A transcript
164 assembled from RNAseq data of the cultivar Coorong matches sequence of both contigs and
165 encodes a full-length CC-NB-LRR protein of 956 amino acids with a single intron within the
166 coding sequence (Fig. 4B). Amplification from the four mutants confirmed the nucleotide
167 changes detected by Renseq in each line. Four additional mutants were also examined by PCR
168 amplification and one (M3) contained a single amino acid change (T211I) in the p-loop while
169 the gene sequence failed to amplify from the other three (M7, M8, M9) indicating that they
170 contained deletions of this region. The eight independent mutants containing deletions or
171 missense mutations in this gene provided strong evidence that it confers *Sr27* resistance.
172 Among known wheat resistance proteins, *Sr27* is most closely related to *Sr13* (90% amino acid
173 identity; Supplementary Fig. 9,10).

174 To confirm the function of the *Sr27* candidate gene, we first used a wheat protoplast
175 transfection assay to co-express the gene with the *AvrSr27* variants identified above as well as
176 the reporter gene luciferase^{27,28}. Recognition of a *Pgt* avirulence protein by the corresponding
177 disease resistance protein in this assay leads to cell death and therefore a reduction in the
178 expression of the co-transformed luciferase reporter gene which is detected by its
179 bioluminescence. Co-expression of the *Sr27* candidate gene with each of the three *AvrSr27*
180 gene variants led to a strong reduction in luciferase activity compared to the *Sr27* or *AvrSr27*
181 genes alone (Fig. 4C). This was a specific recognition response as no loss of reporter gene
182 expression was seen when *Sr27* was co-expressed with the unrelated *Pgt* avirulence gene
183 *AvrSr50*⁶, nor when *AvrSr27-1* was co-expressed with the unrelated wheat resistance gene
184 *Sr50*²⁹. This result also confirmed that the protein encoded by the *avrSr27-3* virulence allele
185 in Pgt21-0 could be recognised by *Sr27* as observed in the virus-mediated protein
186 overexpression assay (Fig. 2B). Likewise, co-expression of *Sr27* and the three *AvrSr27* variants
187 by agrobacterium-mediated transient transformation in *Nicotiana benthamiana* resulted in cell
188 death induction (Figure 4D, Supplementary Fig.11). Lastly, we generated transgenic wheat
189 lines expressing the *Sr27* gene and found that they showed strong resistance to a wheat stem
190 rust isolate avirulent on *Sr27* (Figure 4E and Table S1), but were fully susceptible to strains of

191 leaf rust (*P. triticina*) and stripe rust (*P. striiformis*) (Table S1) confirming that this gene
192 confers specific resistance to stem rust in wheat.

193

194 *Sr27* is effective against Ug99 and other *Pgt* strains causing recent epidemics and could
195 provide effective protection against wheat stem rust, particularly if used in combination with
196 other resistance genes. However, the current *Sr27*-containing wheat line with the rye 3RS
197 translocation introgression have been reported to show a yield penalty³⁰. Therefore it may be
198 necessary to generate smaller 3RS translocation segments in wheat to alleviate this linkage
199 drag effect. This approach was successful for generating smaller segments of the *Thinopyrum*
200 *ponticum* chromosome carrying *Sr26* and *SrB* (now *Sr61*)³¹. Alternatively, *Sr27* may be used
201 as part of a resistance gene cassette in a transgenic approach to provide durable resistance
202 through pyramiding multiple effective resistance genes at a single locus^{3,32}. The feasibility of
203 this approach was recently demonstrated by the generation of transgenic wheat expressing a
204 gene stack of five cloned *Sr* genes²⁸. The identification of *AvrSr27* allows for confirmation of
205 *Sr27* transgene function in such a multi-resistant line through transient protoplast expression,
206 as demonstrated for *Sr50* and *Sr35*²⁸. The *AvrSr27* gene identification also provides the
207 capacity to detect virulence genotypes in *Pgt* populations through sequencing approaches.
208 Together with *AvrSr35* and *AvrSr50*, this represents the beginnings of a molecular diagnostic
209 toolbox for effective prediction of virulence phenotypes of *Pgt* isolates from genotype
210 sequence data. Given the observed role of gene-expression polymorphisms in virulence on
211 *Sr27*, RNA-based detection³³ may be a valuable approach. This work also highlights that field-
212 based expression data as well as genome sequence may be required for accurate phenotype
213 prediction. This would facilitate regional deployment of the most appropriate stem rust
214 resistance genes and their combinations for effective disease control.

215 **METHODS**

216

217 **Rust isolates and plant material**

218 Australian *Pgt* strains Pgt21-0 and 98-1,2,(3),(5),6 have been described previously ^{2,16,34}.
219 Triticale variety Coorong contains *Sr27* ¹¹ while Rongcoo is a line of triticale susceptible to
220 Australian *Pgt* isolates ³⁵. The wheat line CS WRT238.5 contains a 3RS translocation carrying
221 the *Sr27* resistance gene derived from Imperial Rye in the Chinese Spring background ³⁶.
222 Triticale and wheat plants were grown in a growth chamber at 23°C with a 16-hour light period
223 and 50% humidity.

224

225 ***Pgt* virulent mutant selection**

226 Seedlings of the triticale cultivar Coorong at the 2-3 leaf stage (20 pots [15cm] with 6-8 plants
227 per pot) were inoculated with Pgt21-0 (~250 µL) using talc as a carrier (1:4; spores:talc).
228 Inoculated plants were incubated in a humid chamber maintained at 23°C for 48 hrs. After this
229 time plants were moved to glasshouse maintained at 23°C/18°C (day/ night) under natural
230 daylight. Plants were screened twice, at 14 and 20 days post inoculation, for any susceptible
231 infection sites showing large pustule development typical of a susceptible interaction (infection
232 type 3,4). More than 10 mutant pustules were detected and three of these were collected and
233 re-inoculated onto the susceptible wheat line Morocco for amplification in isolation to prevent
234 cross contamination between isolates. After amplification, the virulence of each mutant on *Sr27*
235 was confirmed by reinfection of Coorong plants. One mutant line was tested on the full
236 Australian differential set for *Pgt* and showed an identical virulence profile to Pgt21-0 except
237 for a single additional virulence for *Sr27*. No other isolates virulent on Coorong were present
238 in the laboratory prior to the mutation screen ruling out contamination as a source of the virulent
239 pustules.

240

241 **DNA isolation and sequencing**

242 DNA was extracted from urediniospores of mutant *Pgt* lines as described ¹⁶, quality
243 assessed with a Nanodrop Spectrophotometer (Thermo Scientific, Wilmington, DE) and the
244 concentration quantified using a broad-range assay in Qubit 3.0 Fluorometer (Invitrogen,
245 Carlsbad, CA, USA). DNA library preparation and Illumina sequencing were performed by the
246 Australian Genome Research Facility (AGRF) on the HiSeq2500 (250 bp PE reads, mutants
247 M1 and M2) or MiSeq (300bp PE reads, mutant M3) platforms and about 20 million reads

248 obtained for each isolate. Sequence reads were imported to CLC Genomics Workbench
249 (CLCGW) version 10.0.1 or later (QIAGEN), filtered and trimmed to remove low quality ends,
250 sequencing adapters and low- quality reads (Trim using quality score 0.01, maximum number
251 of ambiguities 2). Reads from the three mutants as well as from the parent Pgt21-0 were
252 mapped to the karyon-phased chromosome level Pgt21-0 reference genome ² using high
253 stringency settings (similarity fraction 0.98 and length fraction 0.95). Variant calling of each
254 sample against the reference was performed using the “Basic Variant Detection” program with
255 parameters: ignore non-specific matches; minimum coverage 10; significance 1.0%; minimum
256 variant count 2; include broken pairs. The program “Compare variants within group” in
257 CLCGW was used to identify variants specific to each sample as well as shared variants. Non-
258 synonymous variants in secreted protein genes were predicted using the CLCGW tool “Amino
259 Acid Changes” and curated manually by visual inspection of read mapping tracks in CLCGW.
260 Read coverage statistics (mean read depth and percent coverage) for annotated genes were
261 extracted using the “Create Statistics for Target Regions” program.

262

263 **Phylogenetic analyses**

264 For whole-genome SNP calling and phylogenetic analysis we used Illumina DNA
265 sequence data from six Australian isolates ¹⁶, seven South African isolates and one Czech
266 isolate ¹⁸ which we previously showed to belong to a single clonal lineage ². FreeBayes v. 1.1.0
267 ³⁷ was used to call biallelic SNP variants across all samples simultaneously using trimmed reads
268 aligned to the Pgt21-0 genome assembly ². VCF files were filtered using vcfFilter in vcflib
269 (v1.0.0-rc1) with the parameters: QUAL > 20 & QUAL / AO > 10 & SAF > 0 & SAR > 0 &
270 RPR > 1 & RPL > 1 & AC > 0. VCF files were converted to multiple sequence alignment in
271 PHYLIP format using the vcf2phylip script
272 (<https://zenodo.org/record/1257058#.XNnE845Kh3g>) and R-package ips/phyloch wrappings
273 (<http://www.christophheibl.de/Rpackages.html>). Phylogenetic trees were constructed using the
274 maximum likelihood criterion in RAxML v. 8.2.1.pthread ³⁸, assuming unlinked loci and using
275 500 bootstrap replicates with a general time reversible model. Convergence and posterior
276 bootstopping (bootstrapping and convergence criterion) were confirmed with the *-I* parameter
277 in RAxML and also with R-packages ape ³⁹, ips/phyloch and phangorn ⁴⁰. Dendrograms were
278 drawn using ggplot2 ⁴¹ and ggbio ⁴² R-packages. For phylogenetic analyses of Sr27 and related
279 resistance proteins, protein sequences were aligned by CLUSTAL and a Maximum likelihood
280 tree constructed using MEGA version X ⁴³.

281

282 **Virus-mediated *in planta* overexpression of candidate AvrSr27 proteins**

283 The *Barley stripe mosaic virus* (BSMV) mediated protein overexpression system known as
284 “BSMV VOX”^{44,45} comprising three T-DNA binary plasmids, pCaBS- α , pCaBS- β and pCa-
285 γ b2A-LIC, was used in this study. The coding sequence of AvrSr27 variants with the first 27aa
286 of the predicted signal peptide excluded and replaced by a single methionine start codon was
287 amplified by PCR using primer pairs 2-210.F and 2-210.R (*AvrSr27-1*, and *AvrSr27-3*) and 2-
288 210.F and 5-210.R (*AvrSr27-2*) (Supplementary Table 2) and cloned into pCa- γ b2A-LIC to
289 generate BSMV:AvrSr27-1, -2, -3. BSMV:mcs4d⁴⁶, which contains 275-bp non-coding
290 sequence corresponding to the multiple cloning site sequence of the vector pBluescript II KS,
291 was included as a negative control. All constructs were verified by Sanger sequencing.
292 Transformation of the BSMV binary plasmids into *A. tumefaciens* strain GV3101 (pMP90) and
293 agroinfiltration into 3-4 week old *N. benthamiana* plants was done as described previously⁴⁷.
294 Sap from the infiltrated *N. benthamiana* leaves was used to mechanically inoculate leaves of
295 two-leaf stage triticale or wheat plants. Post-inoculation plants were maintained in a contained
296 environment room with day/night temperatures of 23°C/20°C at around 65% relative humidity
297 and a 16 hr photoperiod with light intensity of approximately 180 $\mu\text{molm}^{-2}\text{s}^{-1}$. The
298 presence/absence of virus symptoms in subsequently emerged leaves due to systemic infection
299 of the virus was assessed weekly from 7 to 21 days post-infection. The numbers of inoculated
300 plants showing systemic infection symptoms were recorded for each treatment. Each
301 inoculation experiment involved at least 10 individual plants per BSMV VOX construct and
302 was repeated at least once with similar results.

303

304 **Expression analysis**

305 RNA reads from germinated spores and haustorial tissue (100 bp paired-end) of Pgt21-0 were
306 obtained from NCBI BioProject PRJNA253722¹⁶ while reads from an infection timecourse⁶
307 were obtained from NCBI BioProject PRJNA415866. Salmon 1.1.0⁴⁸ was used to align reads
308 to the *Pgt* 21-0 transcripts and to estimate transcript abundances (TPMs) in each sample
309 (salmon index –keepDuplicates and salmon quant –validateMappings). We used tximport and
310 DESeq2⁴⁹ to assess gene differential expression and to obtain the regularized logarithm
311 transformation (rlog). Secreted protein genes showing differential expression ($\text{padj} < 0.1$ and -
312 $1.5 < \log\text{FC} > 1.5$) for at least one time point during infection versus germinated spores were
313 selected with DESeq2 and k-means clustering using Euclidean distance was performed on the
314 relative rlog transformed counts (average rlog for biological replicates) of the 1,352

315 differentially expressed genes in the secretome. Rather than absolute expression we used the
316 amount by which each gene deviates in a specific sample from the gene's average across all
317 samples. For RT-PCR confirmation of expression, RNA was extracted from infected leaves 5
318 days post inoculation using the Qiagen RNAEasy kit and treated with DNase (Turbo DNase
319 kit). One microgram of total RNA was used for 1st strand synthesis with SuperScript III and
320 oligo(dT) (Invitrogen) according to the manufacturer's instructions (20 µl reaction) and diluted
321 to 100 µl in water. PCRs were performed with gene specific primers (Supplementary Table 2)
322 using GoTaq polymerase with following cycles: 95°C 3min; 95°C 30sec, 58°C 40sec, 72°C
323 50sec 29 cycles; 72°C 5min.

324

325 **Isolation of *Sr27* mutants and NLR gene capture sequencing**

326 Seeds of triticale variety Coorong carrying *Sr27* were subject to EMS mutagenesis as described
327 ⁵⁰. In short, 2000 seeds were treated for 12 hrs with 0.3% Ethylmethanesulfonate (EMS) then
328 washed thoroughly with water and sown in large pots (40 seeds per 30cm pot). Single heads
329 from each M1 plant were threshed separately and M2 families from each plant were sown in a
330 tray (30 M2 families per tray) along with resistant and susceptible controls. One-week
331 seedlings were inoculated with Pgt21-0 and scored for their phenotype 2 weeks post
332 inoculation. Seed was harvested from susceptible plants and retested in the following
333 generation by rust inoculation. DNA was extracted from wild-type Coorong triticale and four
334 homozygous susceptible mutants as described ⁵¹. NLR gene capture was performed by Arbor
335 Biosciences (Ann Arbor, USA) following the myBaits protocol with version 2 of the Triticeae
336 bait library available at github.com/steuernb/MutantHunter. Library construction followed the
337 TruSeq RNA Protocol v2. All enriched libraries were sequenced by a HiSeq 2500 (Illumina)
338 using 250 bp paired-end reads.

339

340 **NLR read assembly and identification of mutations**

341 Primary read sequencing data from wild-type and mutants were first trimmed for quality using
342 Trimmomatic v0.38 ⁵² with the parameters
343 *ILLUMINACLIP:novogene_indexed_adapters.fa:2:30:10:8:TRUE, LEADING:28,*
344 *TRAILING:28, MINLEN:20*. Data from wild-type was then *de novo* assembled using CLCGW
345 v11.0.1 with a length fraction of 0.95 and a similarity fraction of 0.98 and the remaining
346 parameters as default. Contigs shorter than 1kb were omitted from the final assembly using a
347 custom script. An annotation of NBS-LRR motifs was created using the program NLR-Parser
348 ²⁵. Trimmed data of each mutant and wild type was mapped to the *de novo* assembly using

349 BWA v0.7.15⁵³. Samtools v1.7.0⁵⁴ was used for processing of resulting SAM files to retain
350 only reads mapping in a proper pair with parameter *-f 2*, then removing duplicates and
351 generating pileup files using parameters *-BQ0* and *-aa*. SNV calling and subsequent candidate
352 identification was performed using the following scripts from the MuTrigo pipeline
353 (<https://github.com/TC-Hewitt/MuTrigo>). Contig regions with high levels of SNPs in the
354 wildtype data indicating poor assembly or read alignment were detected using *Noisefinder.pyc*
355 with default parameters and masked prior to downstream analysis. Potentially mutated
356 nucleotide positions were recorded from pileup files using *SNPlogger.pyc* with parameter *-d*
357 *20*. *SNPtracker.pyc* was used to retrieve contigs containing polymorphisms in two or more
358 mutants using default parameters plus parameter *-s C\>T G\>A indel*. This translates to
359 considering only polymorphisms with a minimum of 80% mutant allele frequency and
360 selecting only for insertions, deletions, or C-to-T or G-to-A SNVs that do not share an identical
361 position with another mutant or wild-type. Candidate gene contigs were aligned to the
362 chromosome scale reference assembly of *Secale cereale* inbred line ‘Lo7’⁵⁵ and the *Triticum*
363 *aestivum* cv. Chinese Spring reference (CSv1) assembly IWGSC RefSeq v1.0²⁶ using BLAST
364 v2.7.1.

365

366 **Confirming the full length candidate *Sr27* sequence**

367 Primers Sr27c5723ExtF1 and Sr27c2413ExtR1 (Supplementary Table 2) were designed based
368 on the genomic sequence of the two non-overlapping contigs #2413 and #5723 and were used
369 to amplify the non-overlapping region between these contigs. A *de novo* RNA transcript
370 assembly was generated from Illumina RNAseq data from Coorong seedlings infected with *Pgt*
371¹⁶ (downloaded from NCBI-SRA SAMN07836894, PRJNA415866) using CLCGW v11.0.1
372 (similarity fraction of 0.98 and the remaining parameters as default). A full-length RNA
373 transcript matching the genomic sequence and including the 5’ and 3’ UTR regions was
374 identified and the primers Sr27F and Sr27R1 were used for amplification for the full-length
375 gene from the wildtype and mutants for subsequent sequence comparison. All PCRs were
376 performed using Phusion high fidelity DNA polymerase (NEB, USA) according to
377 manufacturer’s instructions.

378

379 **Generation of expression constructs**

380 *AvrSr27* gene sequences with the first 27aa of the signal peptide excluded and replaced by a
381 single methionine start codon were amplified from cDNA from purified haustoria of Pgt21-0
382 using Phusion high-fidelity DNA polymerase (Thermo Scientific) and cloned into

383 pENTRTM/D-TOPO[®] according to manufacturer's (Invitrogen) instructions. Full length Sr27
384 cDNA was also cloned into pENTRTM/D-TOPO[®]. For wheat protoplast transfection *Sr27*
385 (coding sequence including introns) and *AvrSr27* sequences were inserted into the p35s-pUbi-
386 GTW-GFP⁵⁶ using Gateway[®] Technology (Life TechnologiesTM). Plasmids encoding GFP
387⁵⁷ and Luciferase²⁷ were previously described. Primers used for PCR are shown in
388 Supplementary Table 2. LR Clonase was used to introduce inserts from entry clones Gateway-
389 compatible pGADT7 and pGBKT7 (Clontech) vectors for yeast-two-hybrid assays⁵⁸, and
390 pAM-PAT vectors^{59,60} for *in planta* transient expression driven by the CaMV 35S promoter.
391 All plasmids were confirmed by sequencing and analysed using Vector NTI Advance (Life
392 Technologies) or CodonCode Aligner V.4.0.4 (CodonCode Corporation) software.

393

394 **Transient expression assays**

395 Wheat protoplast isolation and transformation were performed as described⁵⁷. High quality
396 plasmid DNA was isolated by using Qiagen Endo-free Plasmid Maxi kits (Cat#12362). DNA
397 concentrations were adjusted to a range from 1µg/µl to 4µg/µl and 10 µg of each plasmid was
398 used in co-transformation experiments. After 24 hours incubation in the dark at 23°C, luciferase
399 activity was quantified as described²⁸. *N. benthamiana* plants were grown in a growth chamber
400 at 23°C with 16 h light period. Agrobacterium cultures containing the *Sr27* and *AvrSr27*
401 expression vectors were grown overnight at 28°C in LB media with appropriate antibiotic
402 selections. The cells were pelleted and resuspended in infiltration mix (10 mM MES pH 5.6,
403 10 mM MgCl₂, 150 µM acetosyringone) to an OD₆₀₀ = 0.5 or 1.0, followed by incubation at
404 room temperature for 2 h. Cultures were infiltrated into leaves of 4-week-old tobacco with a 1-
405 ml syringe. For documentation of cell death, leaves were photographed 2-5 days after
406 infiltration

407

408 **Wheat transformation**

409 Scutellum tissue from wheat cultivar Fielder was transformed with Agrobacterium strain
410 AGL0 containing the Ubi-Sr27 construct using hygromycin (30mg/mL) for selection as
411 previously described^{61,62}. T0 lines were screened by PCR with primers Sr27c5723F/R and
412 three positive lines were identified (PC311.3, PC311.17 and PC311.18). T1 seed was harvested
413 and eleven or twelve progeny of each line were grown in a growth cabinet (23°C, 16 h light).
414 Two-week-old seedlings were inoculated with *Pgt* race 98-1,2,(3),(5),6 to which *Sr27* confers
415 resistance, and rust reactions were assessed after 10-15 days. Additional T1 progeny of each

416 line were further tested by inoculation with a leaf rust isolate of pathotype 76-1,3,7,9,10,12,13
417 and a stripe rust isolate of pathotype 134 E16 A+17+33+.

418

419 **References**

420

- 421 1. Singh, R.P., *et al.* Emergence and Spread of New Races of Wheat Stem Rust Fungus:
422 Continued Threat to Food Security and Prospects of Genetic Control. *Phytopathology* **105**,
423 872-84 (2015).
- 424 2. Li, F., *et al.* Emergence of the Ug99 lineage of the wheat stem rust pathogen through
425 somatic hybridisation. *Nature Communications* **10** (2019).
- 426 3. Ellis, J.G., Lagudah, E.S., Spielmeier, W. & Dodds, P.N. The past, present and future of
427 breeding rust resistant wheat. *Frontiers in Plant Science* **5** (2014).
- 428 4. Periyannan, S., Milne, R.J., Figueroa, M., Lagudah, E.S. & Dodds, P.N. An overview of genetic
429 rust resistance: From broad to specific mechanisms. *Plos Pathogens* **13** (2017).
- 430 5. Garnica, D.P., Nemri, A., Upadhyaya, N.M., Rathjen, J.P. & Dodds, P.N. The Ins and Outs of
431 Rust Haustoria. *Plos Pathogens* **10** (2014).
- 432 6. Chen, J., *et al.* Loss of AvrSr50 by somatic exchange in stem rust leads to virulence for Sr50
433 resistance in wheat. *Science* **358**, 1607-1610 (2017).
- 434 7. Salcedo, A., *et al.* Variation in the AvrSr35 gene determines Sr35 resistance against wheat
435 stem rust race Ug99. *Science* **358**, 1604-1606 (2017).
- 436 8. Bakkeren, G. & Szabo, L.J. Progress on Molecular Genetics and Manipulation of Rust Fungi.
437 *Phytopathology* **0**, PHYTO-07-19-0228-IA (2020).
- 438 9. Figueroa, M., Dodds, P.N. & Henningsen, E.C. Evolution of virulence in rust fungi - multiple
439 solutions to one problem. *Curr Opin Plant Biol* **56**, 20-27 (2020).
- 440 10. McIntosh, R.A., Wellings, C.R., Park, R.F. Wheat rusts: an atlas of resistance genes. 1995,
441 Melbourne: CSIRO publications.
- 442 11. McIntosh, R.A., Luig, N.H., Milne, D.L. & Cusick, J. Vulnerability of triticales to wheat stem
443 rust. *Canadian Journal of Plant Pathology* **5**, 61-69 (1983).
- 444 12. Zhang, J., Wellings, C.R., McIntosh, R.A. & Park, R.F. Seedling resistances to rust diseases in
445 international triticales germplasm. *Crop & Pasture Science* **61**, 1036-1048 (2010).
- 446 13. Jin, Y., Pretorius, Z.A. & Singh, R.P. New virulence within race TTKS (Ug99) of the stem rust
447 pathogen and effective resistance genes. *Phytopathology* **97**, S137-S137 (2007).
- 448 14. Olivera, P., *et al.* Phenotypic and genotypic characterization of race TKTF of *Puccinia*
449 *graminis* f. sp. *tritici* that caused a wheat stem rust epidemic in southern Ethiopia in 2013–
450 14. *Phytopathology* **105**, 917-928 (2015).
- 451 15. Olivera, P.D., *et al.* Presence of a Sexual Population of *Puccinia graminis* f. sp. *tritici* in
452 Georgia Provides a Hotspot for Genotypic and Phenotypic Diversity. *Phytopathology* **109**,
453 2152-2160 (2019).
- 454 16. Upadhyaya, N.M., *et al.* Comparative genomics of Australian isolates of the wheat stem rust
455 pathogen *Puccinia graminis* f. sp. *tritici* reveals extensive polymorphism in candidate effector
456 genes. *Frontiers in Plant Science* **5** (2015).
- 457 17. Zhang, J., Zhang, P., Karaoglu, H. & Park, R.F. Molecular Characterization of Australian
458 Isolates of *Puccinia graminis* f. sp. *tritici* Supports Long-Term Clonality but also Reveals
459 Cryptic Genetic Variation. *Phytopathology*™ **107**, 1032-1038 (2017).
- 460 18. Lewis, C.M., *et al.* Potential for re-emergence of wheat stem rust in the United Kingdom.
461 *Communications Biology* **1**, 13 (2018).
- 462 19. Visser, B., *et al.* Microsatellite Analysis and Urediniospore Dispersal Simulations Support the
463 Movement of *Puccinia graminis* f. sp. *tritici* from Southern Africa to Australia.
464 *Phytopathology* **109**, 133-144 (2019).
- 465 20. Visser, B., Herselman, L. & Pretorius, Z.A. Genetic comparison of Ug99 with selected South
466 African races of *Puccinia graminis* f.sp. *tritici*. *Molecular Plant Pathology* **10**, 213-222 (2009).
- 467 21. Lee, W.S., Hammond-Kosack, K.E. & Kanyuka, K. Barley Stripe Mosaic Virus-Mediated Tools
468 for Investigating Gene Function in Cereal Plants and Their Pathogens: Virus-Induced Gene

- 469 Silencing, Host-Mediated Gene Silencing, and Virus-Mediated Overexpression of
 470 Heterologous Protein. *Plant Physiology* **160**, 582-590 (2012).
- 471 22. Qutob, D., *et al.* Copy number variation and transcriptional polymorphisms of *Phytophthora*
 472 *sojiae* RXLR effector genes Avr1a and Avr3a. *PLoS ONE* **4**, e5066 (2009).
- 473 23. Pais, M., *et al.* Gene expression polymorphism underpins evasion of host immunity in an
 474 asexual lineage of the Irish potato famine pathogen. *BMC Evolutionary Biology* **18**, 93 (2018).
- 475 24. Wu, W., *et al.* Flax rust infection transcriptomics reveals a transcriptional profile that may be
 476 indicative for rust Avr genes. *PLOS ONE* **14**, e0226106 (2019).
- 477 25. Steuernagel, B., *et al.* Rapid cloning of disease-resistance genes in plants using mutagenesis
 478 and sequence capture. *Nat Biotechnol* (2016).
- 479 26. Appels, R., *et al.* Shifting the limits in wheat research and breeding using a fully annotated
 480 reference genome. *Science* **361**, eaar7191 (2018).
- 481 27. Saur, I.M.L., Bauer, S., Lu, X.L. & Schulze-Lefert, P. A cell death assay in barley and wheat
 482 protoplasts for identification and validation of matching pathogen AVR effector and plant
 483 NLR immune receptors. *Plant Methods* **15** (2019).
- 484 28. Luo, M., *et al.* A five-transgene cassette confers broad-spectrum resistance to a fungal rust
 485 pathogen in wheat. *Nat Biotechnol* <https://doi.org/10.1038/s41587-020-00770-x> (2020).
- 486 29. Mago, R., *et al.* The wheat Sr50 gene reveals rich diversity at a cereal disease resistance
 487 locus. *Nature Plants* **1** (2015).
- 488 30. Marais, G.F. An evaluation of three Sr27-carrying wheat × rye translocations. *South African*
 489 *Journal of Plant and Soil* **18**, 135-136 (2001).
- 490 31. Mago, R., *et al.* Transfer of stem rust resistance gene SrB from *Thinopyrum ponticum* into
 491 wheat and development of a closely linked PCR-based marker. *Theor Appl Genet* **132**, 371-
 492 382 (2019).
- 493 32. Wulff, B.B., Horvath, D.M. & Ward, E.R. Improving immunity in crops: new tactics in an old
 494 game. *Curr Opin Plant Biol* **14**, 468-76 (2011).
- 495 33. Hubbard, A., *et al.* Field pathogenomics reveals the emergence of a diverse wheat yellow
 496 rust population. *Genome Biology* **16**, 23 (2015).
- 497 34. Park, R.F. Stem rust of wheat in Australia. *Australian Journal of Agricultural Research* **58**,
 498 558-566. (2007).
- 499 35. Singh, S.J. & McIntosh, R.A. Allelism of 2 Genes for Stem Rust Resistance in Triticale.
 500 *Euphytica* **38**, 185-189 (1988).
- 501 36. Acosta, A.C. The transfer of stem rust resistance from rye to wheat. *Dissertation Abstracts* **23**,
 502 34-35 (1962).
- 503 37. Garrison, E. & Marth, G. Haplotype-based variant detection from short-read sequencing.
 504 *arXiv*, 1207.3907 (2012).
- 505 38. Stamatakis, A., Ludwig, T. & Meier, H. RAxML-III: a fast program for maximum likelihood-
 506 based inference of large phylogenetic trees. *Bioinformatics* **21**, 456-463 (2005).
- 507 39. Paradis, E., Claude, J. & Strimmer, K. APE: analyses of phylogenetics and evolution in R
 508 language. *Bioinformatics* **20**, 289-290 (2004).
- 509 40. Heibl, C. PHYLOCH: R language tree plotting tools and interfaces to diverse phylogenetic
 510 software packages. *Available online at: <http://www.christopheibl.de/Rpackages.html>*
 511 (2008).
- 512 41. Wickham, H. ggplot2: elegant graphics for data analysis. 2016: Springer.
- 513 42. Yin, T., Cook, D. & Lawrence, M. ggbio: an R package for extending the grammar of graphics
 514 for genomic data. *Genome Biology* **13**, R77 (2012).
- 515 43. Kumar, S., Stecher, G., Li, M., Nkya, C. & Tamura, K. MEGA X: Molecular Evolutionary
 516 Genetics Analysis across Computing Platforms. *Molecular Biology and Evolution* **35**, 1547-
 517 1549 (2018).

- 518 44. Lee, W.S., Rudd, J.J. & Kanyuka, K. Virus induced gene silencing (VIGS) for functional analysis
519 of wheat genes involved in *Zymoseptoria tritici* susceptibility and resistance. *Fungal Genetics*
520 *and Biology* **79**, 84-88 (2015).
- 521 45. Franco-Orozco, B., *et al.* A new proteinaceous pathogen-associated molecular pattern
522 (PAMP) identified in Ascomycete fungi induces cell death in Solanaceae. *New Phytologist*
523 **214**, 1657-1672 (2017).
- 524 46. Hen-Avivi, S., *et al.* A Metabolic Gene Cluster in the Wheat W1 and the Barley Cer-cqu Loci
525 Determines beta-Diketone Biosynthesis and Glauconsness. *Plant Cell* **28**, 1440-1460 (2016).
- 526 47. Lee, W.S., Rudd, J.J., Hammond-Kosack, K.E. & Kanyuka, K. *Mycosphaerella graminicola* LysM
527 Effector-Mediated Stealth Pathogenesis Subverts Recognition Through Both CERK1 and
528 CEBiP Homologues in Wheat. *Molecular Plant-Microbe Interactions* **27**, 236-243 (2014).
- 529 48. Patro, R., Duggal, G., Love, M.I., Irizarry, R.A. & Kingsford, C. Salmon provides fast and bias-
530 aware quantification of transcript expression. *Nature methods* **14**, 417-419 (2017).
- 531 49. Love, M.I., Huber, W. & Anders, S. Moderated estimation of fold change and dispersion for
532 RNA-seq data with DESeq2. *Genome Biology* **15** (2014).
- 533 50. Mago, R., *et al.* Generation of Loss-of-Function Mutants for Wheat Rust Disease Resistance
534 Gene Cloning. *Wheat Rust Diseases: Methods and Protocols* **1659**, 199-205 (2017).
- 535 51. Mago, R., *et al.* Development of PCR markers for the selection of wheat stem rust resistance
536 genes Sr24 and Sr26 in diverse wheat germplasm. *Theoretical and Applied Genetics* **111**, 496-
537 504 (2005).
- 538 52. Bolger, A.M., Lohse, M. & Usadel, B. Trimmomatic: a flexible trimmer for Illumina sequence
539 data. *Bioinformatics* **30**, 2114-2120 (2014).
- 540 53. Li, H. & Durbin, R. Fast and accurate short read alignment with Burrows–Wheeler transform.
541 *bioinformatics* **25**, 1754-1760 (2009).
- 542 54. Li, H., *et al.* The sequence alignment/map format and SAMtools. *Bioinformatics* **25**, 2078-
543 2079 (2009).
- 544 55. Rabanus-Wallace, M.T., *et al.* Chromosome-scale genome assembly provides insights into
545 rye biology, evolution, and agronomic potential. *bioRxiv*, 2019.12.11.869693 (2019).
- 546 56. Akamatsu, A., *et al.* An OsCEBiP/OsCERK1-OsRacGEF1-OsRac1 Module Is an Essential Early
547 Component of Chitin-Induced Rice Immunity. *Cell Host & Microbe* **13**, 465-476 (2013).
- 548 57. Arndell, T., *et al.* gRNA validation for wheat genome editing with the CRISPR-Cas9 system.
549 *BMC Biotechnology* **19**, 71 (2019).
- 550 58. Bemoux, M., *et al.* Structural and Functional Analysis of a Plant Resistance Protein TIR
551 Domain Reveals Interfaces for Self-Association, Signaling, and Autoregulation. *Cell Host &*
552 *Microbe* **9**, 200-211 (2011).
- 553 59. Cesari, S., *et al.* Cytosolic activation of cell death and stem rust resistance by cereal MLA-
554 family CC-NLR proteins. *Proceedings of the National Academy of Sciences of the United*
555 *States of America* **113**, 10204-10209 (2016).
- 556 60. Cesari, S., *et al.* The rice resistance protein pair RGA4/RGA5 recognizes the Magnaporthe
557 oryzae effectors AVR-Pia and AVR1-CO39 by direct binding. *Plant Cell* **25**, 1463-81 (2013).
- 558 61. Richardson, T., Thistleton, J., Higgins, T.J., Howitt, C. & Ayliffe, M. Efficient Agrobacterium
559 transformation of elite wheat germplasm without selection. *Plant Cell, Tissue and Organ*
560 *Culture (PCTOC)* **119**, 647-659 (2014).
- 561 62. Ishida, Y., Tsunashima, M., Hiei, Y. & Komari, T. Wheat (*Triticum aestivum* L.) Transformation
562 Using Immature Embryos, in *Agrobacterium Protocols, Vol 1, 3rd Edition*. 2015, Springer:
563 New York. p. 189-198.
- 564 63. Sperschneider, J., *et al.* The stem rust fungus *Puccinia graminis* f. sp. *tritici* induces
565 centromeric small RNAs during late infection that direct genome-wide DNA methylation.
566 *BioRxiv*, 469338 (2020).

567
568

569 **Acknowledgements.** Work described here was supported by funding from the 2Blades
570 foundation. JC was supported by a Chinese Scholarship Council (CSC) postgraduate
571 fellowship. JS was supported by an Australian Research Council Discovery Early Career
572 Researcher Award 2019 (DE190100066). KK and VP acknowledge financial support by the
573 Institute Strategic Program Grant ‘Designing Future Wheat’ (BB/P016855/1) from the
574 Biotechnology and Biological Sciences Research Council of the UK (BBSRC). HN-P was
575 supported by USDA-NIFA grant #2018-67013-27819.

576 **Author contributions.** P.N.D. conceptualized the project, acquired funding and supervised the
577 work. N.M.U, R.M., V.P., M.L., A.W., D.O., J.C., J.Z., D.B., M.A. and L.H. acquired
578 experimental data. N.M.U., R.M., J.S., H.N-P., T.H., M.F., K.K., J.G.E, and P.N.D, conducted
579 data analysis. P.N.D. drafted the manuscript and all authors contributed to review and editing.

580 **Competing interests.** The authors declare no competing interests.

581 **Data availability.** All sequence data from this study are available in NCBI under BioProject
582 PRJNA695305 (Sr27 MutRenSeq data) and PRJNA698655 (Pgt21-0 mutants). This includes
583 raw data for Figure 2B, S2 and S8. Figure 3 is derived from raw sequence data available in
584 NCBI BioProject PRJNA253722 and PRJNA415866. All other relevant data is available upon
585 request from the corresponding author.

586 **Code availability.** Scripts and files for MutRenSeq analysis are available at
587 <https://github.com/TC-Hewitt/MuTrigo>.

588

589 **Figure legends**

590 **Fig. 1 *Pgt* mutants with virulence to *Sr27*.**

591 **a**, Rust strains Pgt21-0 and a spontaneous mutant (21m1) selected for virulence on *Sr27* were
592 inoculated onto seedlings of triticale line Coorong containing *Sr27*. Image taken 14 days post
593 inoculation. **b**, Read coverage graphs for chromosome 2B (orange bar) of Illumina DNA
594 sequence reads from Pgt21-0 and three *Sr27*-virulent mutants of Pgt21-0 (21m1, 21m2 and
595 21m3). Y-axis represents absolute read depth (0 to 100). Position on the chromosome is
596 indicated in 1 Mbp intervals from the 5' end with the centromere (CM) position ⁶³ indicated.
597 Approximate sizes of the deleted regions in mutant lines are shown in kbp. **c**, Heat map showing
598 percentage of read coverage for all annotated genes in the *AvrSr27* region of chromosome 2B
599 in Illumina reads from Pgt21-0, the spontaneous mutants 21m1, 21m2 and 21m3, four
600 Australian field isolates (98-1,2,3,5,6; 194-1,2,3,5,6; 34,2,12 and 34,2,12,13) and seven South
601 African isolates (SA-01 to 07). The virulence phenotype of each strain on *Sr27* is indicated,
602 with avirulent isolates listed red and virulent ones in blue. Genes encoding secreted proteins
603 are indicated in bold, and the orange box indicates the two genes included in the deletion region.

604 **Fig. 2 The *AvrSr27* locus encodes two related secreted proteins.**

605 **a**, Schematic of gene arrangement at the *AvrSr27* locus and amino acid alignment of *AvrSr27*
606 protein variants from Pgt21-0. *AvrSr27*-1 and *AvrSr27*-2 are encoded at the avirulence allele
607 on chromosome 2B, while *avrSr27*-3 is encoded at the virulence allele on chromosome 2A.
608 Amino acid sequence (single letter code) of *AvrSr27*-1 is shown with identical residues in other
609 variants indicated by a dot. The predicted signal peptide region is underlined and in bold. **b**,
610 Infection of triticale lines Coorong (contains *Sr27*), Rongcoo (susceptible) and a Coorong
611 derived mutant that has lost *Sr27* (M1) with the *BSMV* expression vector encoding the predicted
612 mature *AvrSr27*-1, -2, or -3 proteins, or containing a non-coding multiple cloning site (empty
613 vector). Representative images of the infection phenotypes are shown for each treatment with
614 the numbers of systemically infected plants out of the total number of plants inoculated under
615 each image. Data represent total numbers from two to four independent experiments each
616 involving 10-12 plants per treatment.

617 **Fig. 3 Differential expression of *AvrSr27* alleles.**

618 **a**, Expression levels of the three *AvrSr27* variants in haustoria and germinated spores of Pgt21-
619 0 and in infected plants at 5, 6, and 7 days post infection. Expression levels were derived from
620 mapping RNAseq reads from each of the tissue types (3 biological replicates) to annotated
621 genes of Pgt21-0 and shown as transcripts per million (y-axis). Significant differences are
622 indicated (* $p < 0.05$; ** $p < 0.01$). **b**, Expression profiling of all secreted proteins of Pgt21-0.
623 Clusters with different expression patterns (numbered 1 to 8) are indicated. Positions of
624 *AvrSr27*, *AvrSr35* and *AvrSr50* are indicated. Blue colour intensity indicates relative expression
625 levels (relative rlog transformed counts; darker colour indicates higher expression) in haustoria
626 (H), germinated spores (GS), and infected leaves 2, 3, 4, 5, 6, or 7 days post infection.

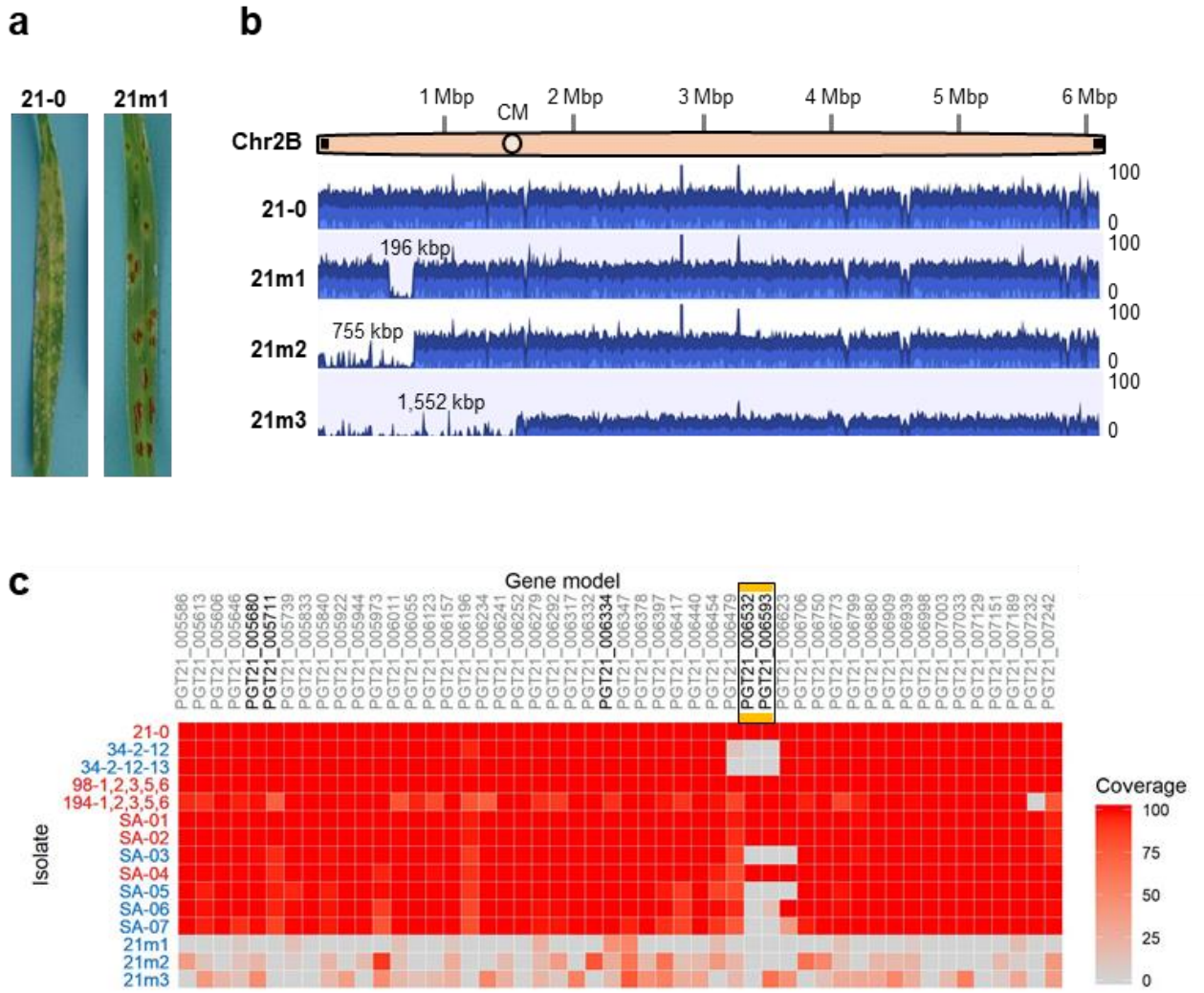
627 **Fig. 4 Identification of the *Sr27* resistance gene.**

628 **a**, Infection phenotype of Coorong (left) and the EMS-derived susceptible mutant #1 (right)
629 inoculated with Pgt21-0 9 days after infection. **b**, Schematic diagram of the *Sr27* protein with
630 the amino acid changes in mutants M1, M3, M4 and M6 indicated. **c**, Luciferase activity
631 (luminescence units y-axis) detected in protoplasts co-expressing *Sr27* or *AvrSr27* variants 1
632 to 3 alone, *Sr27* and *AvrSr27* variants in combination, *Sr50* plus *AvrSr27-1* or *Sr27* plus
633 *AvrSr50*. **d**, Transient expression in *N. benthamiana* of *Sr27*:YFP and YFP:*AvrSr27* variants
634 alone or in combination. YFP alone and the autoactive coiled-coil domain of *Sr50* (CCSr50-
635 YFP) were used as negative and positive controls respectively. Images taken 4 days post-
636 infiltration. **e**, Phenotypes of selected T1 lines and control plants infected with stem rust race
637 98-1,2,3,5,6, and scored 10 days post infection. Image shows an infected leaf from the
638 susceptible Chinese Spring, WRT238.5 containing the native *Sr27* gene, the susceptible parent
639 Fielder and representative T1 plants from two transgenic lines (#3 and #17) containing the *Sr27*
640 transgene and a non-transgenic line recovered from tissue culture (#16).

641

642

643 **Figure 1**



644

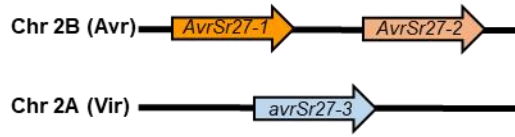
645

646

647

648 **Figure 2**

a



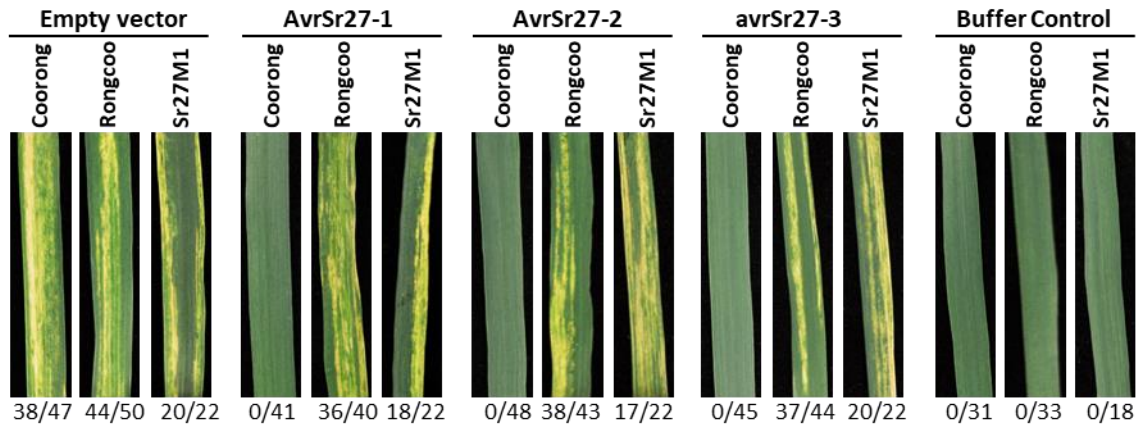
```

AvrSr27-1  MHYITPIILMSIGQFLGILLGAGGLVGAMTPHHQSNCSNPSTLTFPRFI  48
AvrSr27-2  .....K...MI...S.....C.V.VT.T
avrSr27-3  .....D.....I...Y...LT

AvrSr27-1  GKDCSCQLHTKATNLVSVCTSCRKSSLVYEEGSTKGCPCANWHKSTCQEP  96
AvrSr27-2  K.....FN..F..M.....V.....
avrSr27-3  A.....V.....H

AvrSr27-1  KFNRGILSCYCENCQQHTKEKQTISCKNCKNSATTFSHCSSPECHSRW 144
AvrSr27-2  ..E..V.HSL.A...K...ATP.....S.YPY.....R..
avrSr27-3  ..K...HSR.....K..T.....S..PY.....
    
```

b



649

650

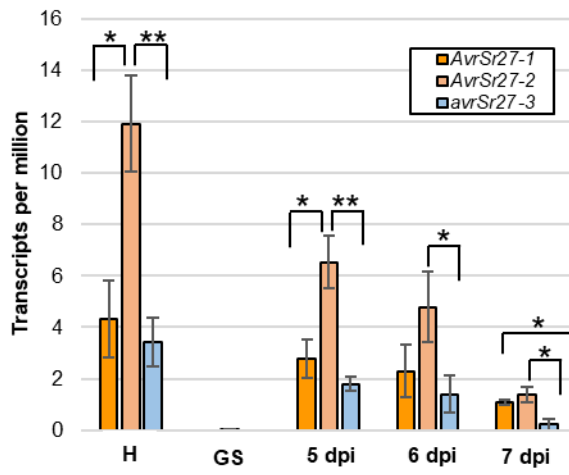
651

652

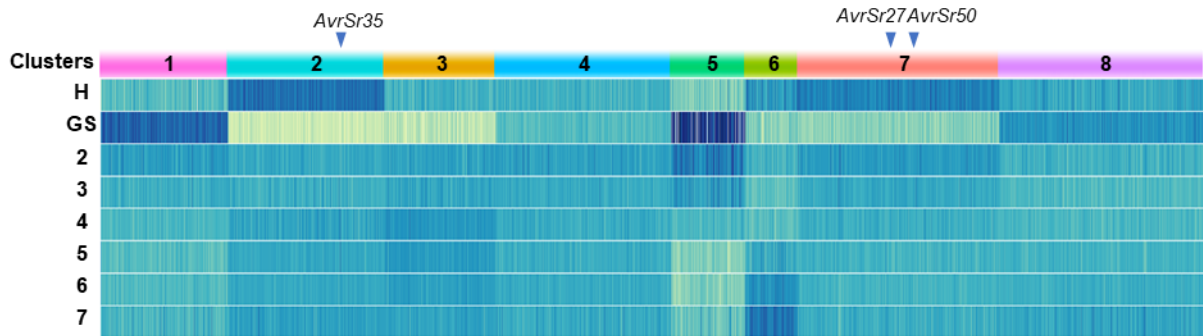
653 **Figure 3**

654

a



b

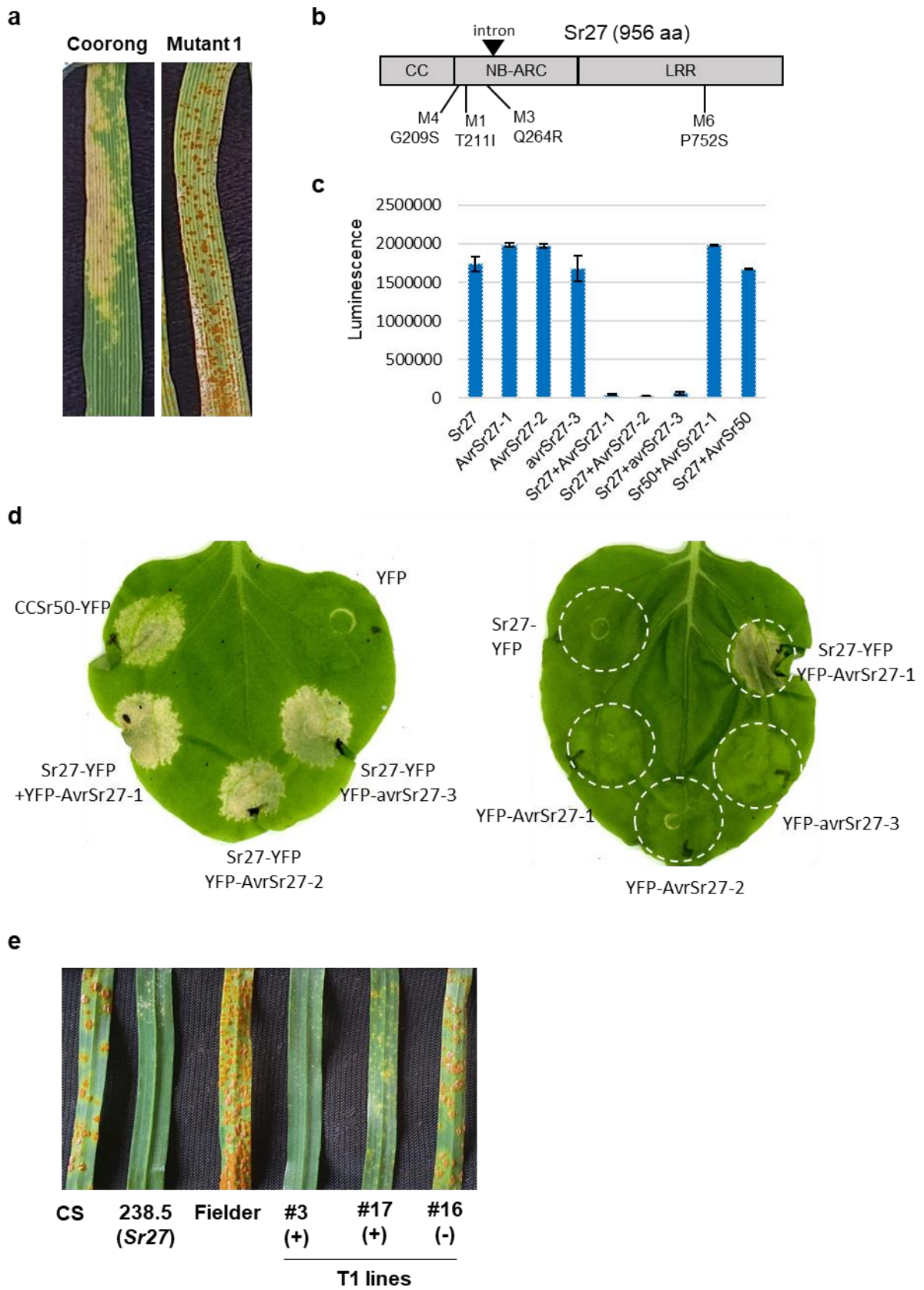


655

656

657

658



662

663

664

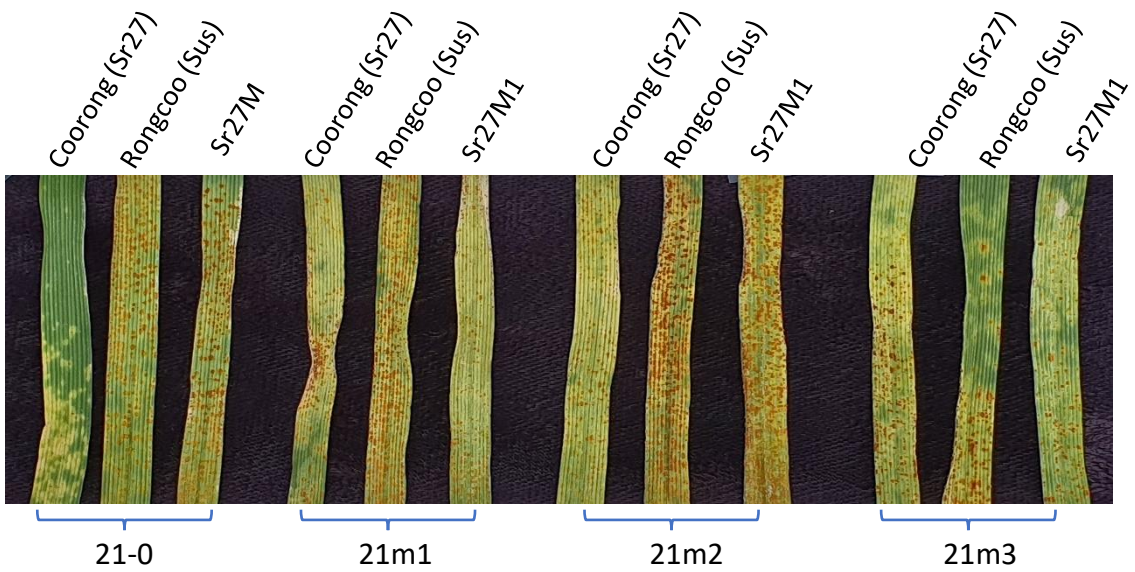


Figure S1 Infection phenotypes of Pgt21-0 and three spontaneous mutants (21m1, 21m2 and 21m3) on Triticale lines Coorong (contains *Sr27*), Rongcoo (rust susceptible) and a mutant line derived from Coorong with a loss of *Sr27* resistance gene (*Sr27M1*). Image was taken 14 days after inoculation of seedling leaves.

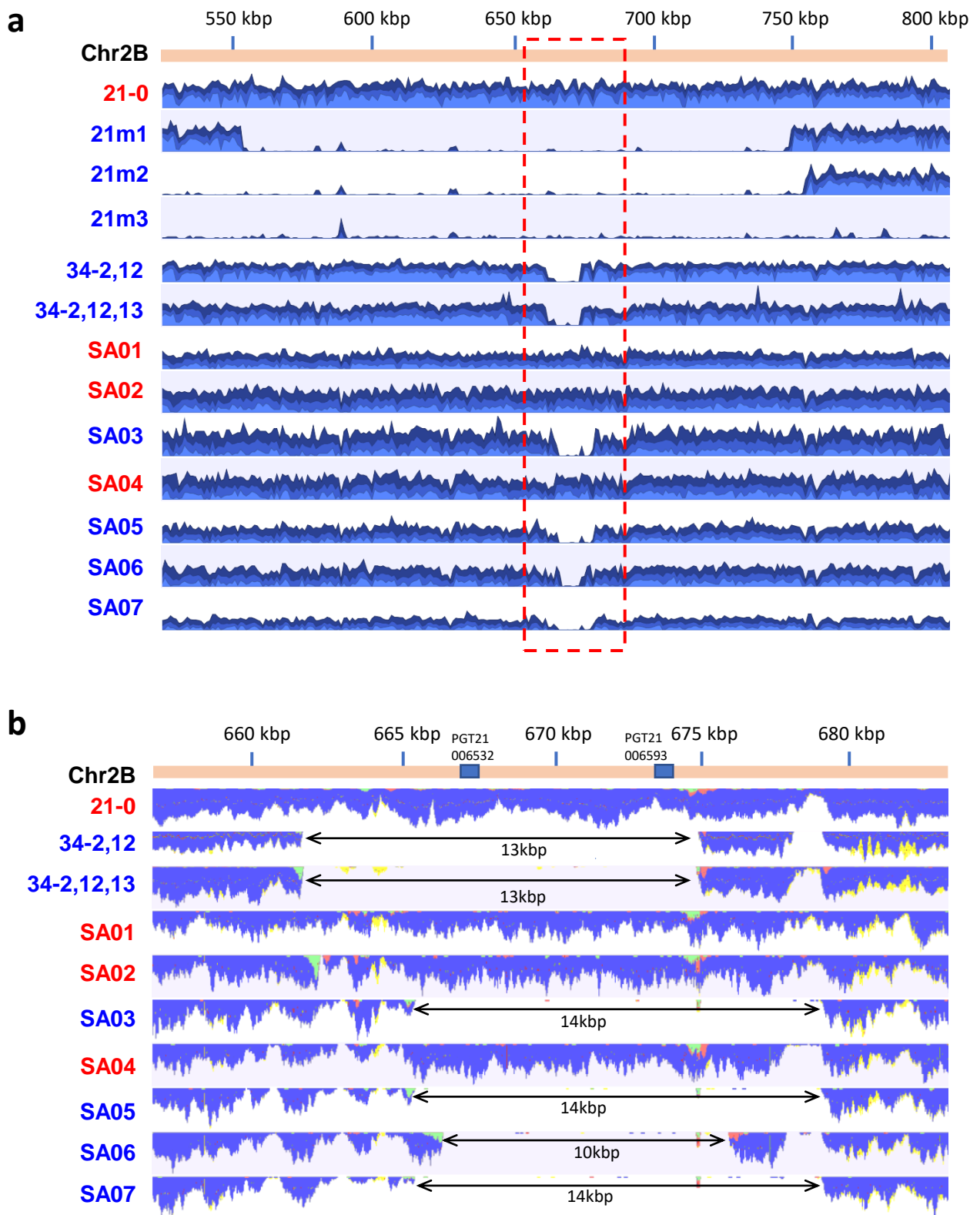
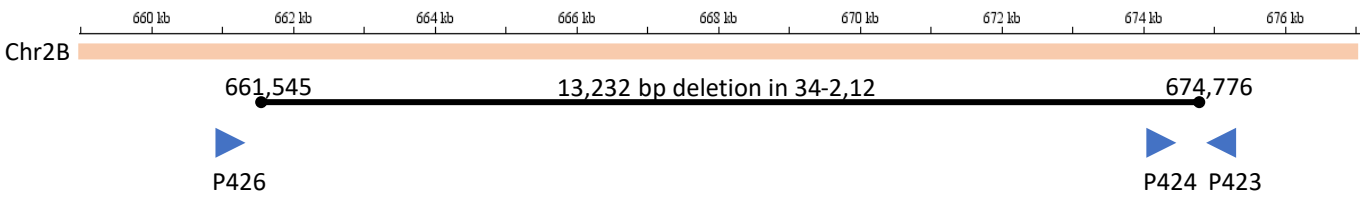


Figure S2 Field isolates of *Pgt* with virulence for *Sr27* contain small deletions on chromosome 2B. **a**, Illumina read coverage graphs for the *AvrSr27* region of chromosome 2B (orange bar) for Pgt21-0, three *Sr27*-virulent mutants of Pgt21-0 and nine field isolates of the same clonal lineage; 34,2,12 and 34,2,12,13 from Australia and SA01 to SA07 from South Africa. Isolates avirulent on *Sr27* are listed in red and virulent isolates in blue. Position on the chromosome in kbp is indicated above the graphs.

b, Close-up of read coverage graphs in boxed region of (A). Approximate sizes of the deleted regions in virulent field isolates are shown in kbp. Positions of Pgt21_006532 and PGT21_006593



Expected amplicon sizes

| | 21-0 | 34-2-12 |
|----------|-------|---------|
| P423/424 | 601bp | -ve |
| P423/426 | -ve | 531bp |
| P383/351 | 380bp | 380bp |

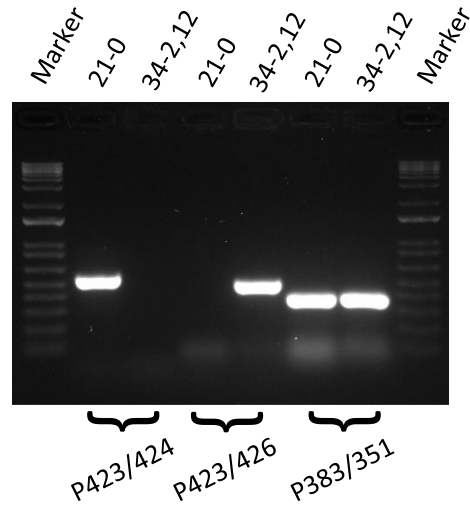


Figure S3 Confirmation of the 13.2 Kbp deletion in *Sr27*-virulent rust strain 34-2-12. The positions of primers P423, P424 and P426 on chromosome 2B around the *AvrSr27* locus are indicated (blue arrow heads) relative to the boundaries of the deletion region in 34-2-12 inferred from the genomic sequence reads. PCR amplification products from genomic DNA of Pgt21-0 and 34-2,12 are shown after separation on a 1% agarose gel. The primers P383 and P351 are designed to amplify a fragment of the *AvrSr50* gene as a control region that is identical in both isolates.

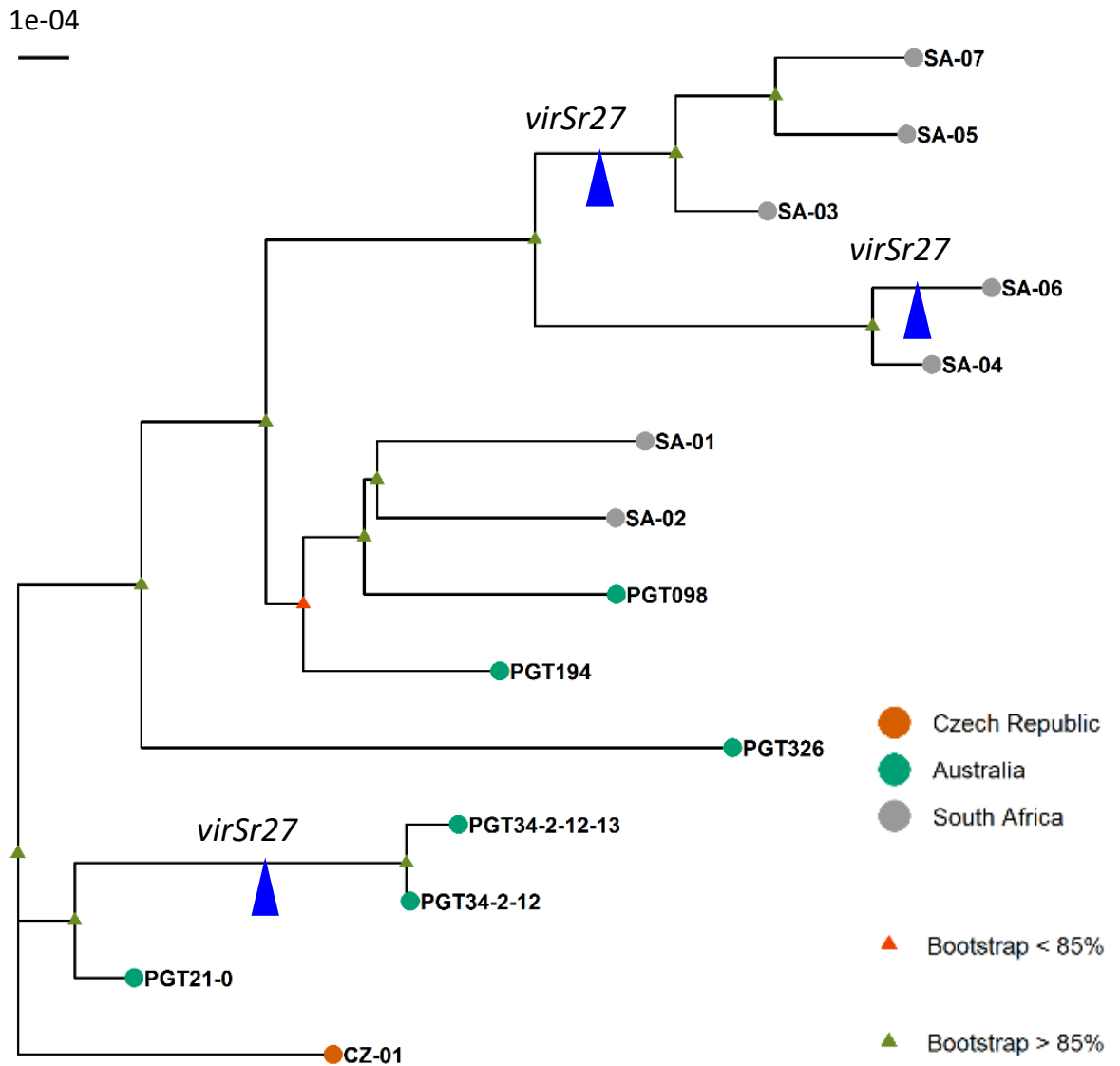


Figure S4 Independent deletions of *AvrSr27* in the race 21 clonal lineage of *Pgt*. Phylogenetic analysis of *Pgt* isolates of the race 21 lineage from South Africa, Australia and the Czech republic (indicated in colour key) using a RAxML model and biallelic SNPs called against the full dikaryotic genome of *Pgt21-0*. Blue arrowheads indicate where three independent mutations leading to virulence on *Sr27* occurred within this lineage. Scale bar indicates number of nucleotide substitutions per site. Nodes with bootstrap values greater than 85% are indicated by green triangles.

a

b

| Construct | WRT238.5 (Sr27) Infection (%) | WRT238.5 (Sr27) n | CS (S) Infection (%) | CS (S) n |
|-----------|-------------------------------|-------------------|----------------------|----------|
| empty | ~92 | 12 | ~83 | 12 |
| AvrSr27-1 | ~1 | 11 | ~73 | 11 |
| AvrSr27-2 | ~1 | 12 | ~75 | 12 |
| avrSr27-3 | ~1 | 12 | ~83 | 12 |

Figure S5 Infection of Triticale lines with BSMV constructs. **a**, RT-PCR assay to check the accumulation BSMV in Coorong, Rongcoo and *Sr27* mutant plants. RNA extracted from leaf samples collected at 14 days post BSMV inoculation was amplified using primers flanking the cloning site in BSMV. +/- indicates the presence or absence of virus symptoms in plants challenged with the respective BSMV construct and buffer control. pDNA of the respective BSMV constructs used as positive control. **b**, Infection of wheat lines Chinese Spring (CS) and CS WRT238.5 (carrying *Sr27* on an introgressed 3RS chromosome segment) with the *BSMV* expression vector encoding *AvrSr27-1*, *-2*, *-3*, or a non-coding multiple cloning site (empty). Y-axis indicates the proportion of inoculated plants that demonstrated systemic viral infection symptoms.

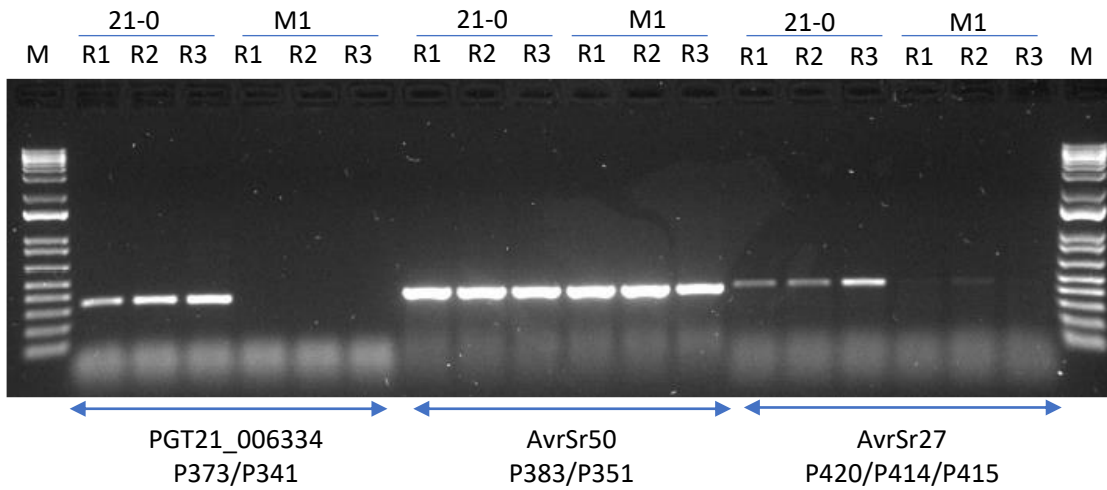


Figure S6 Differential expression of *AvrSr27* alleles. RT-PCR analysis of gene expression in Pgt21-0 and the *Sr27* virulent mutant M1. RT-PCR was performed on three replicate samples (R1 to R3) of RNA extracted from wheat infected with Pgt21-0 or the virulent mutant line (M1). Primers used targeted the transcripts from genes *PGT21-006334* (included in the deleted region of mutant 1, left lanes, primers P373/341), *AvrSr50* (not deleted in mutant 1, middle lanes, primers P383/P351) or all three *AvrSr27* variants (two of which are deleted in mutant 1, right lanes, primers P420/P414/P415).

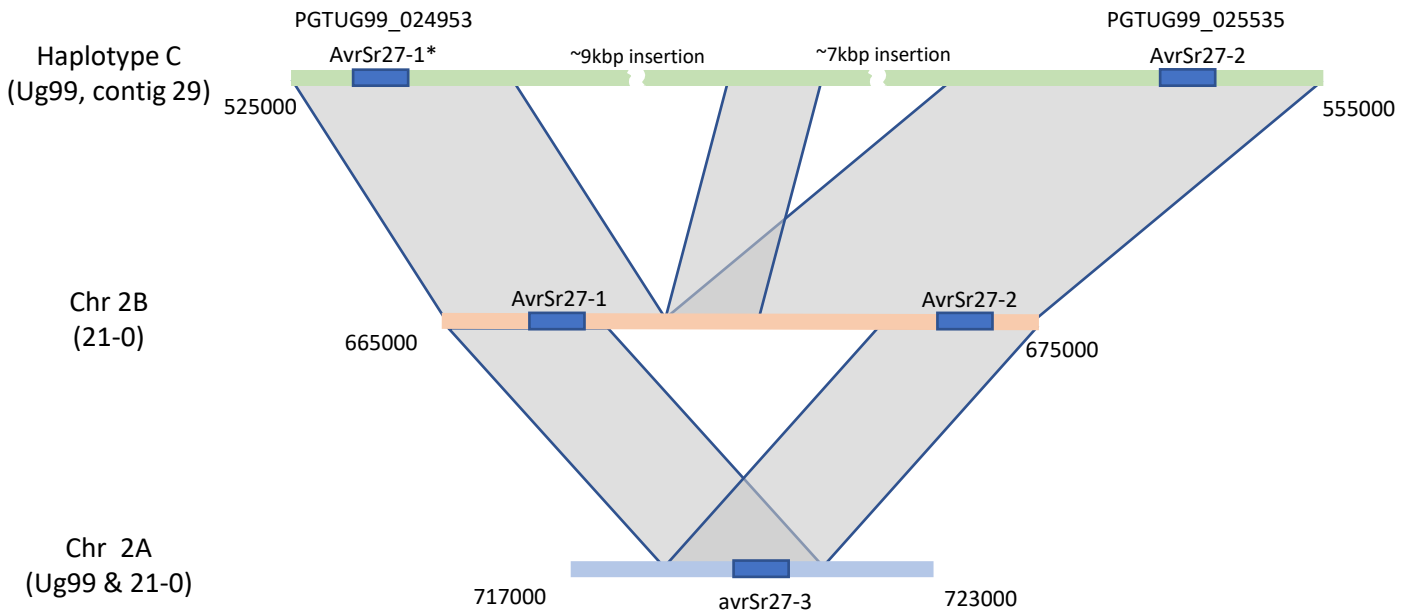


Figure S7 Schematic alignment of *AvrSr27* locus haplotypes from the A, B and C haplotypes (blue, orange and green respectively) of the Pgt21-0 and Ug99 genome assemblies. Regions of high sequence similarity (>95%) between the haplotypes are indicated by grey shading. The positions of *AvrSr27* coding sequences are indicated by the dark blue boxes. *AvrSr27-1** in haplotype C encodes a single amino acid change compared to *AvrSr27-1* on chromosome 2B. Chromosome and contig positions of the selected genome segments are indicated (bp).

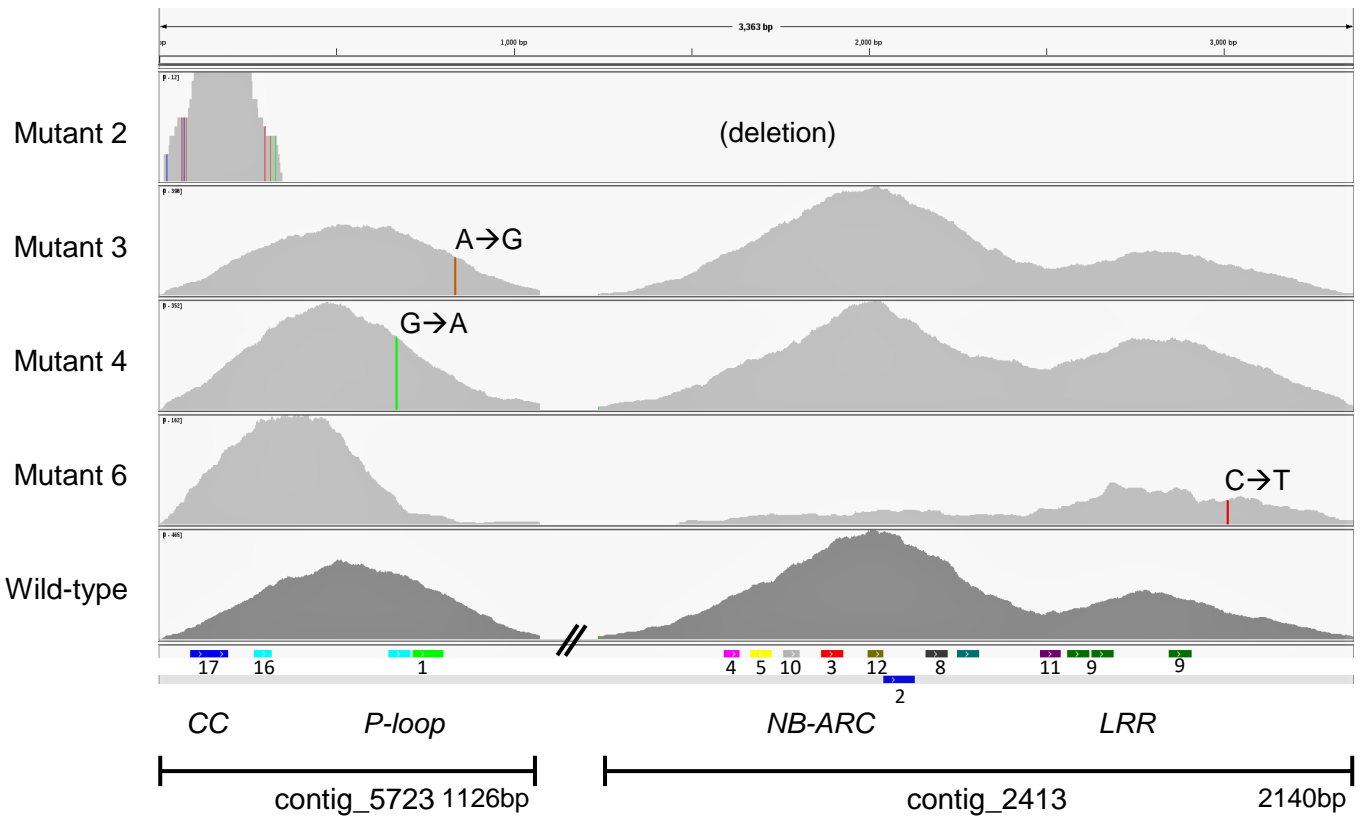


Figure S8 Detection of mutations in a candidate *Sr27* gene by NB-LRR capture and sequencing. Two contigs (#5723 and #2413) assembled from wildtype Coorong contain the 5' and 3' regions of this gene. Read coverage graphs show mapping of reads derived from the NB-LRR capture library from Coorong (wild-type) and four mutants (2,3,4 and 6) to these two contigs. The positions of single nucleotide changes are shown by the coloured bars with the specific change indicated. Mutant M2 produced no reads specific to these contigs and therefore likely contains a deletion. The positions of conserved motifs are indicated under the graphs (numbered colored bars).

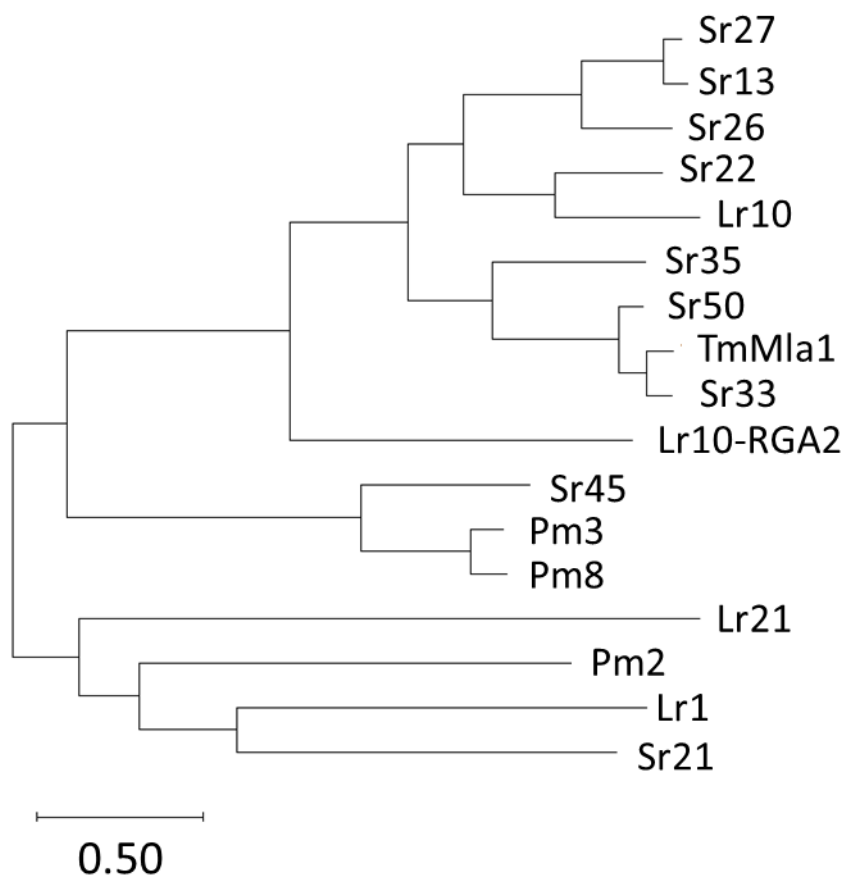
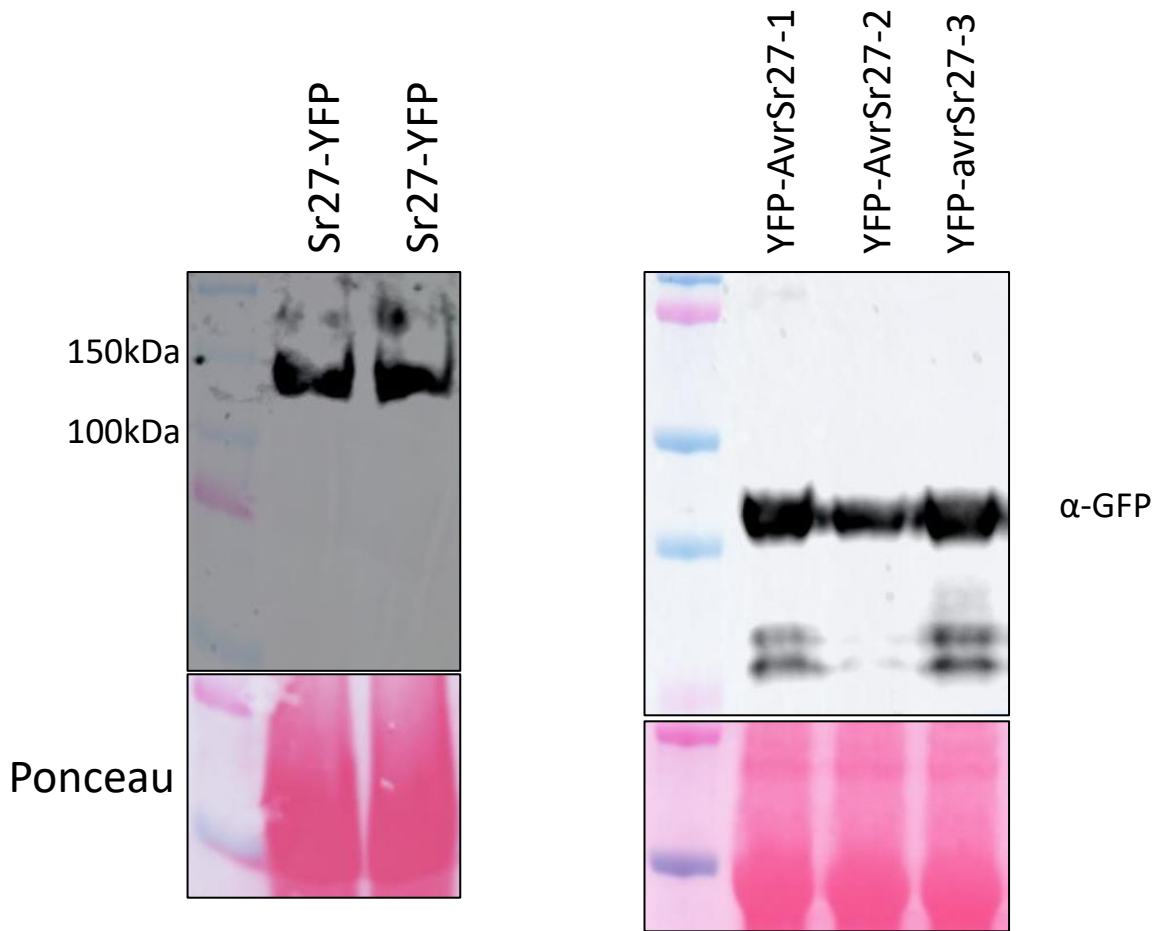


Figure S9 Maximum likelihood phylogenetic tree comparing Sr27 amino acid sequence to proteins sequences of known wheat resistance proteins. Scale bar shows amino acid sequence divergence.

| | | | | | | | | |
|-------|--|-----|-----|-----|-----|-----|--|-----|
| | * | 20 | * | 40 | * | 60 | * | |
| Sr27 | MEAAALVTVATGVLKPVLGKLATLLGDEYKRFKGV | | | | | | IRSLTHELAAMEAFLLKMSEEEEDPDVQDKVVMNEVR | 74 |
| Sr13a | MEAAALVTVATGVLKPVLGKLATLLGDEYKRFKGV | | | | | | IRSLTHELAAMEAFLLKMSEEEEDLNVQDKVVMNEVR | 74 |
| | 80 | * | 100 | * | 120 | * | 140 | |
| Sr27 | ELSYDMEDAIDDFMQSI | | | | | | GDKDEKPDGFTEKIKATLGKLGNMKARHRIGKEIHDLKKQIIEVGDRNARYKGREIF | 148 |
| Sr13a | ELSYDMEDAIDDFMQSVGDKDEKPDGFIDKIKSSLGKLGNMKARHRIGKEIQDLKKQIIEVGDRNARYKGREIF | | | | | | 148 | |
| | * | 160 | * | 180 | * | 200 | * | 220 |
| Sr27 | SKAVNATVDPRALAIFEHASKLVGIDEPKAELIKLLTDE | | | | | | DGVASTQEQVKMVCIVGSGGMGKTTLANQVYQEMK | 222 |
| Sr13a | SKAVNVTVDPRALAI FEHASKLVGIDEPKAELIKLLTDK | | | | | | DGVASTQQQVKMVSIVGSGGMGKTTLANQVYQELK | 222 |
| | * | 240 | * | 260 | * | 280 | * | |
| Sr27 | EEFKFKAFISVSRNPDMN | | | | | | ILRLLSEIIGCQDYAHTTEAGSIQQLISKITDYLAEKRYFIVIDDIWDVKTWDVIK | 296 |
| Sr13a | EKFKCKAFISVSRNPDMT | | | | | | NILRLLSEVIGCQDYADTEAGSIQQLIRKITDYLAEKRYIIVIDDIWDVKTWDVIK | 296 |
| | 300 | * | 320 | * | 340 | * | 360 | * |
| Sr27 | CAFPMTRCGGVIITTTRLSDVAC | | | | | | SCHSSIGGHIYNIRPLNMEHSRQLFYRRLFSSEEDCPSSLVKVSYQILEKC | 370 |
| Sr13a | CAFPMTRCGGVIITTTRLSDVAR | | | | | | SCHSSIGGHIYNIRPLNMEHSRQLFHRRRLFSSEEDCPSSLVKVSNQILEKC | 370 |
| | 380 | * | 400 | * | 420 | * | 440 | |
| Sr27 | DGLPLAIIAIAIGLLANTGRSEHQ | | | | | | WNQVKDSIGRALERNPNSVEVMIKILSLSYFDLPPHLKTCLLYLSIFPEDSI | 444 |
| Sr13a | DGLPLAIIAIAIGLLANTGRSEHL | | | | | | WNQVKDSIGRALERNPNVEVMIKILSLSYFDLPPHLKTCLLYLSIFPEDSI | 444 |
| | * | 460 | * | 480 | * | 500 | * | 5 |
| Sr27 | IEKKTILSRWIAEGFI | | | | | | RQEGRYTAYEVGVRCFNEILVNRSLIQPVKKDDYKGGKSCRVHDIILDFIVSKSIEENFV | 518 |
| Sr13a | IEKKTILSRWIAEGFIQKEGI | | | | | | YTAYEVGVRCFNEILINRSLIQPVKKDDYRGGKSCRVHDIILDFIVSKSIEENFV | 518 |
| | 20 | * | 540 | * | 560 | * | 580 | * |
| Sr27 | TFVGVPSLTTVTQGKVRRLSMQVEEKV | | | | | | DVSILPMSLILSHVRSLNMFEGNTVSIPISEIMELRHLRVLDFGGNRLLEN | 592 |
| Sr13a | TFAGVPSLTTVTQGKVRRLSMQVEGKG | | | | | | DVSILPMSPLILSHVRSFNVERNRVNIHSTMEFRHLRVVDFNDSLL-EN | 591 |
| | 600 | * | 620 | * | 640 | * | 660 | |
| Sr27 | RHLAYVGMILFQLRYLN | | | | | | IYMTAVSELPEQIGHLQCLEMLDIRHTWVSELPASTIANLGKLAHLLISNTGTINVKFP | 666 |
| Sr13a | HHLANVGRLLQLRYLS | | | | | | IYMTAVSELPEQIGHLQCLEMLDIRYTMVSELPASTIVNLGKLAHLLIGSED-TCVKFP | 664 |
| | * | 680 | * | 700 | * | 720 | * | 740 |
| Sr27 | DGIAKMQSLEALHSVNTCN | | | | | | QSYNFLQGLGQLKNLRKLGINIRGVAHEDKEVIASSLGKLCQNLCSLTMW-NDD | 739 |
| Sr13a | DGIAKMQALETLDEVDASK | | | | | | QSYNFLQGLGRKLNLRKLIHIDYHDVAQEDKEVIASSLGKLCQNLCSLTMRGND | 738 |
| | * | 760 | * | 780 | * | 800 | * | |
| Sr27 | DDFLNTWCTSPPLNLRKLV | | | | | | WGCIFFPKVPHWVGSVLNQLKHLLEVGRGTRHEDICILGALPALFTLGLRGSEK | 813 |
| Sr13a | DDFLNTWCTSPPLNLRKLV | | | | | | WGCIFFPKVPHWVGSVLNQLKRLRHVHGKEIRHEDICILGALPALILTGLKGMQK | 812 |
| | 820 | * | 840 | * | 860 | * | 880 | |
| Sr27 | QPSCENRRLAVSGEAGFR | | | | | | CLRKFKYWRWGDWMDLMFTAKCMPRLKLEKLIIFYGHAEDEAPIIPAFDFGIENLSS | 887 |
| Sr13a | QPSCEDGRLAVSGEAGFR | | | | | | CLRKFKYCRWGDWMDLMFTAKCMPKLEKLEKLIIFYRHAQDEAPIIPAFDFGIENLSR | 886 |
| | * | 900 | * | 920 | * | 940 | * | |
| Sr27 | LTTFKCHLGYGPMATKIV | | | | | | DAVKASLDRVVSRAHPNHLTLIFTYCCVFCKSYDCGGRCLLSRDLQSSSEST | 956 |
| Sr13a | LTTFKCHLGC | | | | | | RPMATRTFDAVKASLDRVVRRAHPNHLTVIFSYPLRTSDMTYTFHDCYMRSQD----- | 948 |

Supplementary Fig. 10 Amino acid sequence alignment of the Sr27 and Sr13a resistance proteins.



Supplementary Fig. 11 Immunoblot showing protein expression of Sr27-YFP and YFP-AvrSr27 protein constructs detected using anti-GFP antibodies. Ponceau red staining of filter indicates equal loading of protein extracts.

Supplementary Table 1 Phenotypes of transgenic wheat lines with stem, leaf and stripe rust infection.

| T1 Family | Transgene | Stem rust: 98-1,2,3,5,6 | | | Stripe rust: 134E16A+17+33+ | | | Leaf rust: 76-1,3,7,9,10,12,13+Lr37 | | |
|---------------|-----------|-------------------------|----|----|-----------------------------|---|---|-------------------------------------|---|---|
| | | No. T1 seedlings | R | S | No. T1 seedlings | R | S | No. T1 seedlings | R | S |
| PC311-3 | + | 11 | 11 | 0 | 4 | 0 | 4 | 6 | 0 | 6 |
| PC311-16 | - | 11 | 0 | 11 | 4 | 0 | 4 | 6 | 0 | 6 |
| PC311-17 | + | 12 | 12 | 0 | 5 | 0 | 5 | 5 | 0 | 5 |
| PC311-18 | + | 11 | 10 | 1 | 4 | 0 | 4 | 6 | 0 | 6 |
| PC311-Control | - | 11 | 0 | 11 | 5 | 0 | 5 | 6 | 0 | 6 |

Supplementary Table 2 Primer sequences used

| Primer name | Sequence 5'> 3' | Target |
|----------------|---|--|
| Sr27F | CCTGTTTCGATCACTGGTCG | Sr27 forward |
| Sr27F2 | GTGAAGATGGTCTGCATTGTTGGATCG | Sr27 |
| Sr27R1 | GATGGTATATACCGTGGTCCGACAAAT | Sr27 reverse |
| Sr27R2 | CGGAGGTTAAGCGGCGGAGA | Sr27 |
| Sr27R3 | GGTTTTGTGTGCATAGTTACCAAGAG | Sr27 |
| Sr27c5723F | ATGAACCAAGGCTGAGTTG | Sr27 |
| Sr27c5723R | ACATGCAAAATAGGGCTTCC | Sr27 |
| Sr27c2413F | GTAAGGCTCCAAGGATGCAG | Sr27 |
| Sr27c2413R | TAAGTTTCCCGACGGAATTG | Sr27 |
| Sr27c5723ExtF1 | AAGAACAAGTGAAGATGGTCTGC | Sr27 3' end contig 5723 |
| Sr27c2413ExtR1 | TTCTGTAGAATAGTTGTCTTGAGTGCTC | Sr27 5' end contig 2413 |
| Sr27c2413ExtF1 | TACGAGGAAGCGAAAACAGC | Sr27 |
| Sr27cSeq1R | ATCTTCTCAGTGAAGCCATC | Sr27 |
| Sr27cSeq2R | AAATGTGACTTGATACATCTG | Sr27 |
| Sr27cSeq3F | ATAGTGATTGACGACATATGG | Sr27 |
| Sr27cSeq4F | GATTCATTGCACAAGAAGGT | Sr27 |
| P341 | ATTCAGATTTAAGAGTCTTGATTGAGTCCCCTATG | PGT21_006334 reverse |
| P373 | CACCATGCAATTAGCCAGTGCTTATGTG | PGT21_006334 forward |
| P351 | GTCTTCTCCTACCTGTGTTGGCGCCTTGCAAAATG | AvrSr50 reverse primer |
| P383 | CACCATGATGCATTCAATTATCTTTCAAACACTCC | AvrSr50 forward primer |
| P414 | TTACCATCTTCTGTGACACTCTGGG | AvrSr27-2 reverse |
| P415 | TTACCATCTGCTGTGACACTCTGG | AvrSr27-1/-3 reverse |
| P416 | CACCATGGCAATGACACCACATCACCAAAGCAAT | AvrSr27-1/-2/27 aa signal peptide clipped CDS 5' with CACCATG for directional Topo cloning |
| P417 | CACCATGGCAATGACACCACATCACCAAATCAAT | avrSr27-3/27 aa signal peptide clipped CDS 5' with CACCATG for directional Topo cloning |
| P418 | CCATCTTCTGTGACACTCTGGGCTTG | AvrSr27-2 CDS 3' without stop codon |
| P419 | CCATCTGCTGTGACACTCTGGGCTTG | AvrSr27-1/-3 CDS 3' without stop codon |
| P420 | CACCATGCATTACATCACCCCATATCCTT | AvrSr27-1/-2/-3 forward |
| P423 | AAGTGGATAACGTACTCTGCACAAC | upstream of 5' deletion boundary in 34M1/34M2 mutants |
| P424 | AGTGACTGCAATTCACCAATATTTTCG | Internal to deletion region in 34M1/34M2 mutants |
| P426 | AACATTCAAGTGCAGGAATGGGGAG | downstream of 3' boundary region in 34M1/34M2 mutants |
| 2-210.F | CCAACCCAGGACCGTTGATGGCAATGACACCACATCACAAA | Amplification of AvrSr27-1, -2, and -3 for cloning into BSMV VOX vector |
| 2-210.R | AACCACCACCACCGTTACCATCTGCTGTGACACTCTG | Amplification of AvrSr27-1 and -3 for cloning into BSMV VOX vector |
| 5-210.R | AACCACCACCACCGTTACCATCTTCTGTGACACTCTGG | Amplification of AvrSr27-2 for cloning into BSMV VOX vector |